

UNIVERSITÉ DU QUÉBEC À MONTRÉAL

MISE EN PLACE PAR REMPLACEMENT ET DÉFORMATIONS POST-
VOLCANIQUES DE L'AMAS SULFURÉ À ZN-CU ARCHÉEN DE
PERSÉVÉRANCE, DISTRICT MINIER DE MATAGAMI, QUÉBEC

MÉMOIRE
PRÉSENTÉ
COMME EXIGENCE PARTIELLE
DE LA MAÎTRISE EN SCIENCES DE LA TERRE

PAR
SAMUEL PIERRE

JUIN 2014

UNIVERSITÉ DU QUÉBEC À MONTRÉAL
Service des bibliothèques

Avertissement

La diffusion de ce mémoire se fait dans le respect des droits de son auteur, qui a signé le formulaire *Autorisation de reproduire et de diffuser un travail de recherche de cycles supérieurs* (SDU-522 – Rév.01-2006). Cette autorisation stipule que «conformément à l'article 11 du Règlement no 8 des études de cycles supérieurs, [l'auteur] concède à l'Université du Québec à Montréal une licence non exclusive d'utilisation et de publication de la totalité ou d'une partie importante de [son] travail de recherche pour des fins pédagogiques et non commerciales. Plus précisément, [l'auteur] autorise l'Université du Québec à Montréal à reproduire, diffuser, prêter, distribuer ou vendre des copies de [son] travail de recherche à des fins non commerciales sur quelque support que ce soit, y compris l'Internet. Cette licence et cette autorisation n'entraînent pas une renonciation de [la] part [de l'auteur] à [ses] droits moraux ni à [ses] droits de propriété intellectuelle. Sauf entente contraire, [l'auteur] conserve la liberté de diffuser et de commercialiser ou non ce travail dont [il] possède un exemplaire.»

AVANT-PROPOS

Ce mémoire est rédigé sous la forme d'un article scientifique qui sera soumis à la revue *Economic Geology* sous le titre *Syn-Volcanic Replacement and Post-Depositional Deformation of the Archean Perseverance Volcanogenic Massive Sulfide Deposit, Matagami Mining District, Quebec, Canada*. Sa présentation est différente des mémoires habituellement présentées à l'UQAM. Notamment, la langue de rédaction est l'anglais et les figures et tableaux sont situés à la fin de l'article. Michel Jébrak, directeur de maîtrise, Stéphane Faure, co-directeur ainsi que Gilles Roy (Glencore Canada Corporation) sont co-auteurs de cet article. Ce format de mémoire a été choisi car il donne l'opportunité de transmettre de nouvelles connaissances à la communauté scientifique à l'échelle internationale.

REMERCIEMENTS

Mes premiers remerciements vont à Michel Jébrak, mon directeur de maîtrise. Son enthousiasme permanent, ses multiples idées ainsi que sa généreuse confiance ont permis cet accomplissement professionnel et personnel.

Je tiens aussi à remercier Stéphane Faure, mon co-directeur de maîtrise, pour l'initiation de ce projet, son soutien et son suivi continu des travaux de recherche.

Les équipes de géologues de Matagami, avec en premier lieu Gilles Roy, Réjean Dussault, Julie Drapeau, Richard Nieminen, Roger Brassard, Michel Dessureault et Mélanie Gagnon sont grandement remerciés pour les innombrables discussions sur la géologie du district, leur partage de connaissances et leur appui constant sur le terrain. Je souhaiterais remercier Michelle Laithier pour la réalisation des illustrations, Raynald Lapointe pour ses multiples appuis techniques, ainsi que Jim Franklin, Jeffrey Hedenquist et Alain Tremblay pour l'amélioration de la version initiale du manuscrit.

Je souhaite ajouter un grand merci à ma famille pour son soutien, ainsi qu'à mes amis et collègues de travail, Nico, Sacha, Émilie, Christophe, Noémie, Ludo, Clyde et Adelphine pour cette formidable ambiance de groupe à Montréal.

Ce travail n'aurait pas été possible sans le soutien financier de Glencore Canada Corporation, Donner Metals, Mitacs Accélération, Consorem et Divex.

TABLE DES MATIÈRES

AVANT-PROPOS	ii
LISTE DES FIGURES.....	v
LISTE DES TABLEAUX.....	vi
RÉSUMÉ.....	vii
INTRODUCTION GÉNÉRALE	1
CHAPITRE 1	
SYN-VOLCANIC REPLACEMENT AND POST-DEPOSITIONAL DEFORMATION OF THE ARCHEAN PERSEVERANCE VOLCANOGENIC MASSIVE SULFIDE DEPOSIT, MATAGAMI MINING DISTRICT, QUEBEC, CANADA.....	4
Abstract	4
1.2 Regional Geologic Setting	7
1.3 Sampling and Analytical Methods	10
1.4 Geology of the Perseverance Deposit	12
1.4.1 General stratigraphy	12
1.4.2 Lithofacies.....	13
1.4.3 Mineralization and alteration	15
1.4.4 Metal zonations	17
1.5 Alteration Geochemistry	18
1.5.1 Lithogeochemistry.....	18
1.5.2 Alteration indexes	19
1.5.3 Precursor selection and mass balance calculations	19
1.5.4 Mapping of mass balance results	20
1.6 Structural Geology	22
1.6.1 Host-rock setting	22
1.6.2 Massive sulfide structures	24
1.6.3 Mineral fabrics	27
1.7 Discussion	28
1.7.1 Evidence for subseafloor replacement	28
1.7.2 Post-volcanic deformation overprint.....	31
1.8 Conclusion.....	36
Acknowledgments.....	37
References	38
CONCLUSION GÉNÉRALE	59
APPENDICE A	
MODÉLISATION 3D DU GISEMENT DE PERSÉVÉRANCE	61
BIBLIOGRAPHIE	71

LISTE DES FIGURES

Figure	Page
1.1 Geologic map of the Matagami district.....	44
1.2 Surface geologic map of the Perseverance deposit.....	45
1.3 Geologic sections of the Equinox and Perseverance-West orebodies	46
1.4 Photographs of ore and alteration facies at Perseverance	47
1.5 Metal distributions of the Equinox and Perseverance-West orebodies.....	49
1.6 Discrimination diagrams of the Perseverance volcanic rocks.....	50
1.7 Plan views of mass balance calculations in the volcanic sequence	51
1.8 Lower hemisphere equal-area projection of structural fabrics.....	53
1.9 Photographs and microphotographs of structural elements in the deposit.....	54
1.10 Mechanical behavior of base-metal sulfides during metamorphism.....	56
1.11 Schematic model of the Perseverance deposit history	57

LISTE DES TABLEAUX

Tableau	Page
1.1 Geochemical compositions of the volcanic units and their precursors	58

RÉSUMÉ

Persévérence est un amas sulfuré volcanogène de taille moyenne (5,1 millions de tonnes (Mt)) et de haute teneur (15,8% Zn, 1,24% Cu, 29,4 g/t Ag, 0,4 g/t Au), localisé dans le district de Matagami, au nord de la ceinture de roches vertes archéenne de l'Abitibi. Le gisement comprend quatre lentilles de sulfure massif, encaissées dans la portion supérieure d'une séquence rhyolitique massive, la rhyolite de Watson. Les quatre lentilles sont entièrement discordantes par rapport à une séquence volcanique de faible pendage (20° NW) et sont entourées d'une intense altération proximale en chlorite (\pm talc). Le toit des lentilles est constitué d'un horizon de tuf finement laminé utilisé comme marqueur stratigraphique, la Tuffite Clé, ainsi que d'une unité de rhyodacite, la rhyodacite de Dumagami.

Des calculs de bilan de masse à Persévérence indiquent la présence de forts enrichissements en MgO (supérieurs à 10% poids) associés à un lessivage en K₂O et en Na₂O (jusque -4% poids respectivement) dans le mur ainsi que dans le toit du gisement. Ces résultats sont en accord avec des valeurs élevées des indices d'altération (e.g., indice chlorite-carbonate-pyrite (CCPI), indice d'altération index (AI)) et témoignent d'une altération pervasive en chlorite dans le toit du gisement avec une intensité et une géométrie similaires à ce qui est enregistré dans le mur. Outre les altérations dans le toit du gisement, la présence de nombreuses reliques de l'encaissant dans le minéral ainsi que la relation discordante existant entre les enveloppes minéralisées et la stratigraphie, suggèrent que le gisement de Persévérence s'est formé par remplacement sous fond marin.

Les roches felsiques encaissantes sont affectées par une schistosité pénétrative le long de laquelle les quatre enveloppes minéralisées sont globalement co-planaire et aplatis. La présence de plis serrés dans la Tuffite Clé montre que la séquence volcanique est déformée dans les zones d'intense chloritisation proches des lentilles. La plupart des structures et des textures présentes dans le minéral sont le résultat de déformations et de recristallisations, incluant notamment un rubanement vertical dans les sulfures, un boudinage important et des structures de type percement et durchbewegung. Les contrastes de résistance des matériaux, associés à leur ductilité, contrôlent largement la déformation à Persévérence et ont une influence importante sur la géométrie, le tonnage ainsi que la teneur du gisement. Le comportement relativement ductile de la chalcopyrite suggère que le minéral a été remobilisé au sein des lentilles et que la distribution en cuivre dans le gisement est reliée à des mécanismes de déformation post-volcaniques.

La présence d'amas sulfurés formés par remplacement sous fond marin dans le district de Matagami implique la possibilité d'utiliser les enrichissements en Mg ainsi que le lessivage en éléments alcalins dans le toit des horizons fertiles comme outil d'exploration. Les contrastes de rhéologie des matériaux génèrent une corrélation spatiale entre les zones d'altération et la focalisation de la déformation malgré l'absence de relation génétique, créant ainsi un guide structural pour la recherche d'amas sulfurés.

MOTS CLÉS: Amas sulfuré, Persévérance, Abitibi, remplacement syn-volcanique, déformation, contraste de compétence

INTRODUCTION GÉNÉRALE

Le district minier de Matagami, situé au nord de la ceinture de roches vertes archéenne de l'Abitibi dans le craton du Supérieur, a produit 49,6 millions de tonnes (Mt) de minerai entre 1963 et 2013, incluant 4,6 Mt Zn et 0,44 Mt Cu (G. Roy, pers. commun., 2014) et représente le second district zincifère archéen en Abitibi après Timmins. Les amas sulfurés du district sont cités comme un exemple classique de mise en place exhalative dans un contexte de fond marin (Lavallière et al., 1994; Ioannou et Spooner, 2007; Ross et al., 2014). Cette interprétation se fonde principalement sur la relation spatiale étroite qui existe entre les gisements et le marqueur stratigraphique régional qu'est la Tuffite Clé. En dehors du flanc nord du district qui est reconnu pour son important caractère structural (Piché et al., 1993), le flanc sud - hébergeant la majorité des gisements découverts - est quant à lui reconnu comme étant faiblement déformé (Lavallière et al., 1994; Ioannou et Spooner, 2007). Cependant, de récentes réinterprétations sur la nature de la Tuffite Clé (Genna et al., 2014) ainsi que la reconnaissance de facteurs structuraux contrôlant certains gisements du flanc sud (Roberts, 1975) soulignent que ces points sont encore sujet à débats. La compréhension de la genèse de ces gisements ainsi que des déformations postérieures les ayant affectés est cruciale pour de futures explorations dans le district et dans des environnements similaires car ils contrôlent la géométrie, le tonnage et potentiellement la teneur des cibles recherchées.

Le gisement de Persévérence est localisé dans la partie nord-ouest du district, au sein du flanc sud (Fig.1.1) et est défini par des ressources pré-production de 5.1 Mt à 15.8% Zn, 1.24% Cu, 29.4 g/t Ag et 0.4 g/t Au (Arnold, 2006). Persévérence est constitué de quatre lentilles caractérisées par des géométries verticales et perpendiculaires à une séquence volcanique de faible pendage (20° NW). Cet environnement est atypique pour le district, où les gisements ont soit une forme d'amas dans une séquence à pendage modéré (e.g., Matagami Lake: Roberts, 1975),

soit une forme tabulaire dans une séquence à fort pendage (e.g., Isle-Dieu: Piché et al., 1993 and Bracemac-McLeod: Adair, 2009). L'environnement de Persévérence constitue un contexte favorable à la distinction des processus synvolcaniques par rapport aux processus postérieurs à la mise en place enregistrés au cours de l'histoire géologique. Un ensemble de textures et de caractéristiques enregistrées au sein du gisement de Persévérence fournissent l'évidence d'une formation de style remplacement sous fond marin. Il est aussi démontré qu'une reprise structurale importante est enregistrée au sein des lentilles et des roches encaissantes - en relation avec le métamorphisme régional aux schistes verts - et a un impact sur la réorientation des lentilles minéralisées ainsi que sur une remobilisation interne des sulfures.

L'objectif de ce projet de recherche est d'approfondir la compréhension métallogénique du gisement de Persévérence, en déterminant les contrôles de mise en place de la minéralisation ainsi que l'impact des déformations survenues après celle-ci. La géochimie des altérations, la cartographie structurale de détail ainsi que la caractérisation microscopique du minerai sont utilisés afin de reconstruire l'interaction étroite entre les éléments syn- et post-volcaniques enregistrés par la minéralisation et son environnement immédiat. Après la mise en contexte de la problématique du projet de recherche, sont respectivement présentés la géologie régionale du district de Matagami ainsi que la géologie locale du gisement de Persévérence. S'ensuivent un volet d'étude de la géochimie des altérations incluant un calcul de bilan de masse par sélection des précurseurs ainsi qu'un volet concernant la géologie structurale du gisement au niveau de la minéralisation et des roches encaissantes. Il est ensuite discuté de l'environnement probable de mise en place de la minéralisation à Persévérence -par remplacement sous fond marin- ainsi que des modifications d'ordre structural apportées après l'épisode de volcanisme. Ces interprétations sont étendues dans la conclusion à l'échelle du district de Matagami avec un apport aux méthodes d'exploration des amas sulfurés du secteur. En annexe, un volet consacré à la

modélisation 3D du gisement de Persévérence à l'aide du logiciel Leapfrog 3D® est présenté. Bien que n'apportant que pas d'éléments supplémentaires à la compréhension du gisement, la modélisation permet de visualiser la relation entre l'ensemble des éléments le constituant, tel que les unité de la séquence volcanique, les lentilles minéralisées (leur nature et leur teneur en Cu-Zn) ainsi que les résultats géochimiques obtenus par la méthode du bilan de masse.

Ce mémoire est présenté sous forme d'un article scientifique qui sera soumis dans une revue spécialisée traitant de la géologie économique. L'article a été rédigé par le premier auteur. Le second auteur est Michel Jébrak, directeur de maîtrise, dont l'implication a consisté en la génération de pistes de recherche et en leur suivi, à l'aide sur le terrain ainsi qu'à la relecture de l'article. Le troisième auteur est Stéphane Faure, co-directeur de maîtrise, à l'origine du projet de recherche et dont l'implication a été identique à celle du second auteur. Le quatrième auteur, Gilles Roy, est également à l'origine du projet de recherche du côté du partenaire industriel et dont l'implication a consisté en un soutien logistique sur le terrain, au suivi scientifique du projet ainsi que son financement.

CHAPITRE 1

SYN-VOLCANIC REPLACEMENT AND POST-DEPOSITIONAL DEFORMATION OF THE ARCHEAN PERSEVERANCE VOLCANOGENIC MASSIVE SULFIDE DEPOSIT, MATAGAMI MINING DISTRICT, QUEBEC, CANADA

Abstract

Perseverance is a medium size (5.1 million metric tons (Mt)), high-grade (15.8% Zn, 1.24% Cu, 29.4 g/t Ag, 0.4 g/t Au) volcanogenic massive sulfide (VMS) deposit located in the Matagami district of the northern Abitibi greenstone belt. The deposit comprises four massive sulfide lenses hosted within the upper part of a >1500 m-thick rhyolite, the Watson rhyolite. Ore envelopes are characterized by pipelike geometries discordant to a low-dipping volcanic sequence and are surrounded by intense proximal chlorite (\pm talc) alteration. The hanging wall of the lenses is constituted by a regional stratigraphic marker of finely laminated tuff, the Key Tuffite, and by a >200 m-thick coherent rhyodacitic unit, the Dumagami rhyodacite.

Mass balance calculations at Perseverance indicate strong MgO enrichments (exceeding 10 wt%) associated to K₂O and Na₂O depletions (down to -4 wt% respectively) in both the footwall and hanging wall rocks of the deposit. These results, together with high alteration index values (e.g., chlorite-carbonate-pyrite index (CCPI), alteration index (AI)) indicate a pattern of pervasive chlorite alteration in hanging wall rocks with very little change in intensity and geometry to that present in the footwall. In addition to intense alteration in the hanging wall, the presence of abundant host-rock relicts within the ore and the discordant relationship between the ore envelopes and bedding suggest that the Perseverance deposit formed dominantly by subseafloor replacement.

The four orebodies of Perseverance and their surrounding host rocks display evidence for strong post-depositional deformation. The host felsic rocks are affected by a penetrative schistosity, along which the four flattened orebodies are globally co-planar. Tights folds in the Key Tuffite unit show that the volcanic sequence is deformed, with maximum deformation in zones of intense chlorite alteration adjacent to the orebodies. Most of the fabrics and textures in the ore are the result of combined deformation and recrystallization and include a structural banding in the sulfides, strong boudinage, piercement and durchbewegung structures. Contrasting ductilities of the materials largely control the deformation at Perseverance and play a significant role for the shape, tonnage and grade of the deposit. In particular, the relatively ductile behavior of chalcopyrite suggests that the mineral was remobilized within the orebodies and that the present copper distribution in the deposit is largely related to post-volcanic deformation mechanisms.

The presence of subseafloor-replacement style VMS deposits in the Matagami district suggests a careful examination of Mg enrichments and alkali depletions within the hanging walls of fertile horizons during exploration programs. Rheology contrasts between materials generate a spatial correlation between alteration zones and the focus of deformation despite the lack of a genetic relationship, thus creating a structural footprint for VMS localization.

KEYWORDS: VMS deposit, Abitibi, syn-volcanic replacement, deformation, copper remobilization, rheology contrasts

1.1 Introduction

The Matagami mining district in the northern Abitibi greenstone belt of the Superior Craton, Canada, has produced 49.6 million metric tons (Mt) of ore from 1963 to 2013, including 4.6 Mt Zn and 0.44 Mt Cu (G. Roy, pers. commun., 2014) and constitutes the second most important Archean zinc district in Abitibi after Timmins. Volcanogenic massive sulfide (VMS) deposits of the district are often quoted as a classical example of exhalative-style mineralization in a seafloor setting (Lavallière et al., 1994; Ioannou and Spooner, 2007; Ross et al., 2014). This interpretation is mainly based on the close spatial relationship existing between the deposits and the regional stratigraphic marker known as the Key Tuffite. Besides the North Flank of the district (Fig. 1.1) that is recognized for its strong structural overprint (Piché et al., 1993), the South Flank of the district - where most of the deposits are hosted - is generally noted for its weak deformation (Lavallière et al., 1994; Ioannou and Spooner, 2007). However, recent reinterpretations on the nature of the Key Tuffite unit (Genna et al., 2014) and previous recognition of structural singularities in at least one of the deposits of the South Flank area (e.g., Matagami Lake: Roberts, 1975) indicate that these points are controversial. Comprehension of the genesis and subsequent structural modifications of these deposits is critical for future exploration in the district and in other similar environments as they control the shape, tonnage and grade of desired targets. In the present study, the combination of geochemistry and detailed structural mapping at the Perseverance deposit is employed to reconstruct the close relationship existing between the syn-volcanic and post-depositional components of these deposits.

The Perseverance deposit is located in the northwestern part of the district, within the south flank area (Fig. 1.1) and is defined by premining resources of 5.1 Mt at 15.8% Zn, 1.24% Cu, 29.4 g/t Ag and 0.4 g/t Au (Arnold, 2006). Perseverance comprises four vertical pipelike massive sulfide bodies that are perpendicular to a low dipping (20° NW) volcanic sequence (Fig. 1.2). This setting is atypical for the district, where the deposits are either mound-shaped in a moderately dipping sequence (e.g.,

Matagami Lake: Roberts, 1975) or tabular-shaped in a steeply dipping sequence (e.g., Isle-Dieu: Piché et al., 1993 and Bracemac-McLeod: Adair, 2009). It further represents a favorable framework to distinguish the syn-volcanic versus post-depositional elements that are recorded in the geologic evolution. A series of textures and features present in the Perseverance deposit provide evidence in favor of a formation by subseafloor replacement. It is also demonstrated that a significant post-volcanic deformational overprint is recorded in the orebodies and their immediate host rocks - in relation with regional greenschist facies metamorphism - and has an impact on the reorientation of the ore envelopes as well as on internal sulfide remobilizations.

1.2 Regional Geologic Setting

The Matagami mining district (Fig. 1.1) is located 250 km north of Rouyn-Noranda in the early Archean Abitibi subprovince, within the northernmost volcanic sequence of the Abitibi greenstone belt. A total of 20 volcanogenic massive sulfide deposits ranging in size from ~0.1 to >25 Mt (e.g., Matagami Lake) has been discovered in the district, of which 13 have been put into production. The deposits are typically zinc-rich, averaging ~9 wt% Zn, and contain as much as 18.7 wt% Zn (e.g., Isle-Dieu). Numerous studies have contributed to the geologic understanding of the district, with regional descriptions by Sharpe (1968), Beaudry and Gaucher (1986), Piché et al. (1993) and Filote et al. (2011).

Stratigraphy in the district consists of a lower, dominantly felsic volcanic assemblage, the Watson Lake Group, overlain by a dominantly mafic volcanic assemblage, the Wabassee Group. The Watson Lake Group comprises: 1) a lower poorly exposed, >500 m-thick, Fe-rich tholeiitic dacite (Liagh and MacLean, 1992; Piché et al., 1993) and 2) an upper, >1500 m-thick, massive tholeiitic rhyolite (the

Watson rhyolite), dated at 2725.9 ± 0.8 Ma_{U-Pb} (Ross et al., 2014). Both units display evidence of submarine volcanic emplacement, with hyaloclastites, autobreccias and pillow lavas (Beaudry and Gaucher, 1986; Arnold, 2006).

A thinly laminated tuffaceous unit, the Key Tuffite, marks the transition to the Wabassee Group and can be traced across the entire district with a thickness ranging between a few centimeters and ten meters. Most of the zinc-rich volcanogenic massive sulfide deposits of the district are located at this interface and the unit represents a stratigraphic marker used as a first-order vector for exploration. Long time interpreted to be largely exhalative in composition, the Key Tuffite is now considered as a homogeneous calc-alkaline andesitic tuff, marking the transition with the andesitic rocks of the overlying Wabassee Group (Liaghat and MacLean, 1992; Genna et al., 2014). The Wabassee Group consists of thick flows of light-colored massive and pillowed calc-alkaline andesites and minor dark pillowed tholeiitic basalts (MacLean, 1984; Liaghat and MacLean, 1992). This mafic-dominated assemblage is locally interfingered with felsic units, represented by the >200 m-thick Dumagami rhyodacite (2725.4 ± 0.7 Ma_{U-Pb}; Ross et al., 2014) and the 25 to 60m-thick Bracemac rhyolite (2725.8 ± 0.7 Ma_{U-Pb}; Ross et al., 2014).

Both the Watson Lake and Wabassee Groups are locally intruded by late phases of the underlying Bell River complex, a large (>5000 m-thick) tholeiitic gabbro-anorthosite layered intrusion dated at $2724.6 +2.5/-1.9$ Ma_{U-Pb} (Mortensen, 1993). Several authors, including Maier et al. (1996), Ioannou and Spooner (2007) and Carr et al. (2008) have suggested that the Bell River complex acted as a heat source to drive hydrothermal circulation at the origin of VMS deposits. Geochemical similarities with the Watson Lake and Wabassee Group tholeiitic basalts suggest that these lithologic units were derived through fractionation processes associated with the Bell River Complex (MacGeehan and MacLean, 1980). A bulk of the Bell River Complex is interpreted as having emplaced prior to and/or during VMS formation (Maier et al., 1996, Ioannou and Spooner, 2007).

Postvolcanic intrusions of varying compositions (dioritic, tonalitic, granodioritic) occur throughout the district and include the Radiore gabbroic serie (2720 ± 1 Ma_{U-Pb}; Mortensen, 1993), the Olga Lake pluton (2693 ± 1.6 Ma_{U-Pb}; Mortensen, 1993). In addition, Proterozoic diabase dikes intrude the stratigraphy throughout the western part of the camp (Piché et al., 1993).

Volcanic rocks of the region have undergone greenschist facies metamorphism and are affected by the Galinée anticline, a broad-scale, northwest-plunging structure that separates the district into the north flank and the south flank areas (Fig. 1.1). Two stages of deformation are recorded in the region of Matagami, resulting from north-south convergence and from the collision between the Abitibi and Opatica subprovinces to the north (Beaudry and Gaucher, 1986; Pilote et al., 2011). The main deformation is represented by a steeply dipping, northwest-southeast trending schistosity (S₁) in association with regional pluri-kilometric folds, including the Galinée anticline. A second phase of deformation (D₂), documented in the north flank of the district, crosscuts the S₁ fabric and is defined by an east-west trending schistosity (S₂) and small-scale folds (F₂) with steep plunges dipping towards the south (Beaudry and Gaucher, 1986). The south flank stratigraphy is displaced by a northwest-southeast-trending high-angle reverse fault, the Daniel fault, with a 500 m vertical thrust on the northern block, as calculated from seismic reflection interpretation (Adam et al., 1998). A generation of late transverse faults striking between N30° and N45° also crosscuts the volcanic sequence along the south flank (Fig. 1.1).

The north flank is characterized by an east-west-trending stratigraphy steeply dipping towards the north. This area displays a high level of deformation with strongly foliated and flattened rocks along numerous anastomosing shears subparallel to the lithological trend. Regional metamorphism in the north flank locally reaches middle amphibolite facies east of the Bell River (Beaudry and Gaucher, 1986; Piché

et al., 1993). VMS deposits of the north flank are strongly deformed and most of the orebodies display vertically flattened shapes (e.g., Norita: Piché et al., 1993). In contrast, the south flank is described as weakly deformed (Piché et al., 1993, Lavallière et al., 1994; Ross et al., 2014), with variable southward to westward dips increasing from 20° in the vicinity of the Perseverance deposit to a maximum of 60° close to the Bracemac-McLeod deposit. Deformation in the south flank is interpreted to be minimal and confined to narrow brittle-ductile shear zones with no structural impact on VMS deposits of the area (Lavallière et al., 1994; Arnold, 2006).

1.3 Sampling and Analytical Methods

Data used for the alteration geochemistry study are supplemented by 2807 whole rock geochemical analyses from Glencore Canada Corporation, corresponding to 231 exploration and delineation drill holes conducted on the Perseverance property. Analyses were performed at the Chimitec commercial laboratory located in Vancouver, British Columbia for major oxides and trace elements using the X-ray fluorescence method. Thirty-nine complementary samples were collected underground for comparison and representation of the various lithologies with their corresponding alterations. ALS Minerals performed analyses on those samples at Val d'Or, Quebec, using fusion ICP-AES for major oxides elements and fusion ICP-MS for trace elements.

A total of 1711 whole rock analyses were used for mass balance calculations including 1066 samples of the Watson rhyolite and 645 samples of the Dumagami rhyodacite. Absolute mass changes were calculated for mobile elements based on the dilution or concentration of immobile components, through the equation of Gresens (1967). The mass of a sample after alteration (reconstructed composition, R.C.) was calculated from the initial chemical analysis on the basis of 100 mass units (mass

units and wt% values are interchangeable) of precursor rocks, using TiO_2 as the immobile monitor:

$$\text{R.C.} = \text{TiO}_2 \text{ precursor} / \text{TiO}_2 \text{ altered} \times \% \text{ component}_{\text{altered}}$$

Mass change for each mobile element is calculated as:

$$\text{Mass Change} = \text{R.C.} - \text{Precursor Composition}$$

Mass changes for the Watson rhyolite and the Dumagami rhyodacite were independently calculated with their respective precursor compositions (Table 1) for the following mobile major elements: CaO , Fe_2O_3 , K_2O , MgO , MnO , Na_2O and SiO_2 . The grids were produced using an inverse distance weighting method on Mapinfo-Discover with a linear weighting model, four nearest neighbours and two gridding passes.

The sections illustrating Cu and Zn distributions were obtained from the block model resource estimate of the Perseverance feasibility study (resource estimate: Arnold, 2006). Three-dimensional block models were constructed by ordinary kriging interpolations for Equinox, Perseverance-Main and Perseverance-West. The models were constrained with 7966 base metal assays at 1 m intervals performed at the Chimitec commercial laboratory located in Vancouver, British Columbia by atomic absorption spectroscopy (AAS) for Zn, Cu, Pb and Ag. Assay quality assurance and quality controls were carried out for base metals using the Falconbridge Drill Core Sampling and Analysis Protocol. Copper and zinc sections for Equinox and Perseverance-West (Fig. 1.5a and b) are based on blocks of 2.5 m-side with a thickness of one block.

Structure, lithology and alteration were mapped in 18 underground drifts of the 70, 95, 105 and 130 levels of the Perseverance deposit. Structural data were analyzed on rose plots and lower hemisphere equal area stereonets.

1.4 Geology of the Perseverance Deposit

Perseverance is the northwestern-most polymetallic volcanogenic massive sulfide deposit discovered in the south flank of the Matagami mining district. With premining resources of 5.1 Mt grading 15.8% Zn, 1.2% Cu, 29.4 g/t Ag and 0.4g/t Au (Arnold, 2006), it constitutes the second richest deposit of the district in terms of average zinc grade, after Isle Dieu (i.e., 18.7% Zn: Lavallière et al., 1994) and ranks second in terms of tonnage after Matagami Lake (i.e., 25.6 Mt: Roberts, 1975). The Perseverance deposit is composed of four distinct orebodies occurring within an area of 800 x 500 m: Equinox, Perseverance-West, Perseverance-Main and a smaller satellite lens, Perseverance-2 (Fig. 1.2). The discovery results from a diamond drilling program designed to test airborne EM/Mag geophysical anomalies in an area considered to be favourable by its prospective geology (Arnold, 2006).

1.4.1 General stratigraphy

The four massive sulfide lenses of Perseverance occur at and below the contact between the footwall Watson rhyolite and the hanging wall Dumagami rhyodacite (Fig. 1.3a, b). They present a pipelike shape and are entirely discordant to their near-horizontal host volcanic sequence, which dips at ~20° towards the northwest (Fig. 1.3a,b). A low-dipping volcanic sequence contrasts with the rest of the district where greater dips are generally observed (i.e., subvertical dips in the north flank and elevated dips elsewhere along the south flank). Displacement along a series of west-northwest late brittle-ductile faults, such as the New Hosco fault (Fig. 1.2), is believed to be responsible for the preservation of this near-horizontal stratigraphy (Arnold, 2006). Most deposits of the Matagami district are either mound-shaped in a moderately dipping sequence (e.g., Matagami Lake: Roberts, 1975) or tabular-shaped in a steeply dipping sequence (e.g., Isle-Dieu: Piché et al., 1993 and Bracemac-McLeod: Adair, 2009). The atypical morphology and environment of the

Perseverance orebodies thus constitute a particularity in the district.

1.4.2 Lithofacies

The Watson rhyolite constitutes the footwall to the Perseverance deposit and hosts the four orebodies within its upper 200 m section (Fig. 1.3a, b). Primary volcanic textures are preserved in the rhyolite, including abundant hyaloclastic breccias, flow banding and columnar jointing (Beaudry and Gaucher, 1986; Piché et al., 1993). Spherulites are locally abundant and indicate a formation from supercooled melt close to the glass transition or a devitrification of the lava. The rhyolite varies from aphyric to porphyritic with millimeter-sized quartz and albite phenocrysts set in a groundmass of microcrystalline quartz, plagioclase and chlorite. Characteristic centimeter-sized amygdules filled with quartz and chlorite constitute 5 to 10 % of the rock volume.

In Perseverance, the Key Tuffite is present at the interface between the Watson rhyolite and the Dumagami rhyodacite. Its thickness is variable in the vicinity of the four orebodies and ranges between ~20 cm and 3 m. The Key Tuffite is commonly exposed at the upper extremity of the orebodies and generally overlies the massive sulfides (Equinox: Fig. 1.3a). In many cases however, the unit can be traced below the stratigraphic top of the lenses, with significant portions of ore crosscutting it (Fig. 1.3, 1.4e). The primary structures of the Key Tuffite, such as its thin depositional laminations, are commonly obliterated by a pervasive black magnesian chlorite alteration (Fig. 1.4a). In Perseverance, the Key Tuffite unit is almost completely devoid of sulfides away from the proximal alteration halo surrounding the orebodies. This lack of sulfides in the Key Tuffite is unusual for a deposit of the south flank area, where the unit typically contains 1.5 to 2 wt% Zn as well as variable percentages of pyrite (Arnold, 2006).

The overlying Wabassee Group in the vicinity of Perseverance is represented by the Dumagami rhyodacite. Along with the Key Tuffite, this >200 m-thick unit forms the hanging wall to the four orebodies (Fig. 1.3a, b). Primary volcanic textures are preserved in the rhyodacite, including hyaloclastic breccias and columnar jointing. Large (1-5 mm) plagioclase spherulites can locally constitute up to 80% of the rock volume and it was noted that their abundance increases in contact zones, such as the one overlying the Key Tuffite unit. Total thickness of the Dumagami rhyodacite is unknown in the vicinity of Perseverance and the unit is bounded by faults to the south and to the north. Although true lateral and vertical extension of the Dumagami rhyodacite can't be constrained, this coherent unit presents great variations in thickness apparently correlated with a central depression in the deposit, which possibly reflects the presence of a rhyodacite dome. The dominantly felsic nature of the Perseverance host rocks constitutes an exception in the district, where most of the deposits are associated to an overlying mafic hanging wall (e.g., andesites of the Matagami Lake (Roberts, 1975) and Norita deposits (Piché et al., 1993).

Dikes and intrusions of different compositions are common in the deposit and intrude both the volcanic sequence and the massive sulfide orebodies. The oldest generation is characterized by several dikes of tonalite with plagioclase phenocrysts and spherulites in a fine-grained chloritized groundmass (Arnold, 2006). A 10 to 30 m-thick dike of tonalite, with a moderate dip toward the south crosscuts the volcanic sequence between the Perseverance-Main and Perseverance-2 orebodies. Tholeiitic gabbro dikes constitute a second generation of intrusions across the deposit with thicknesses varying from a few centimeters to several tens of meters. A major tholeiitic gabbro sill subconcordant to the stratification can be followed in cross section immediately above the Equinox orebody (Fig. 1.3a). The sill is probably connected with vertical feeders present in the orebody (Arnold, 2006). Tholeiitic gabbro units are fine-grained, massive and typically strongly hydrothermally altered in and around the orebodies. Previous dike generations are in turn crosscut by a

family of calc-alkaline intermediate dikes across the deposit and characterized by an average thickness of ~1 m; they are typically greenish, massive with a fine-grained texture and are affected by hydrothermal alteration. Two later generations of calc-alkaline monzonite and lamprophyre dikes also intrude the sequence with an average thickness of 5 m and are not hydrothermally altered. Lamprophyre dikes generally strike northwest and have shallow northerly dips (Arnold, 2006).

1.4.3 Mineralization and alteration

Mineralization: In the Perseverance deposit, mineralization occurs in the Equinox, Perseverance-West, Perseverance-Main and Perseverance-2 zones and is dominated by Zn-Cu rich massive sulfides with variable amounts of base metal-poor pyritic sulfides (Fig. 1.4). The mineralization consists of a variety of facies, identical throughout the different orebodies, and include the followings: (1) stringer sulfides occurring within chlorite-rich peripheric zones, (2) chalcopyrite- and sphalerite-rich massive sulfides, (3) banded massive sulfides, (4) massive pyritic sulfides with minor sphalerite and chalcopyrite, and (5) lenticular masses of magnetite. Stringer sulfides consist of fine-grained to granular pyrite with lesser chalcopyrite and sphalerite, and constitute ~10 to 50 vol % of the rock at the base and in the periphery to the orebodies. These stringers grade into massive sulfides in the upper portion of the orebodies, where pyrite, sphalerite, chalcopyrite, varying proportions of pyrrhotite and minor galena represent up to 90 to 95 vol % of the volume. Fragments of variably altered rhyolite and gangue minerals are locally common within the massive sulfides (Fig. 1.4b). Banded sulfides consist of dominant pyrite with varying proportions of sphalerite and chalcopyrite that form mm- to cm-thick bands (Fig. 1.4c). Magnetite is present throughout the massive sulfides in varying percentages (Fig. 1.4d) and also occurs as massive lenses. A 25 m-thick magnetite zone is developed at the base of the Perseverance-Main orebody and shares several similarities with the magnetite zone

described at the Ansil deposit by Galley et al. (1995). The different facies are generally closely associated in space with gradual transitions from one to the other, excepted for the lenticular masses of magnetite that are associated to sharp contacts.

Although largely enclosed within the Watson rhyolite, significant portions of ore locally crosscut the Key Tuffite at the top of the orebodies and are in direct contact with the hanging wall Dumagami rhyodacite, (Fig. 1.4e). The vertical extension of ore above the Key Tuffite is estimated to range between a few meters and up to several tens of meters (Fig. 1.3a, b).

Alteration: VMS hydrothermal alteration is highly developed in the volcanic rocks of the Perseverance deposit. Altered rocks consist predominantly of chlorite, variable proportions of talc, minor sericite and quartz.

In the footwall Watson rhyolite, alteration is particularly marked and increases from unaltered to weakly altered ~150 m from mineralization, to intensely altered proximal to mineralization (i.e., within 25 m). Black magnesian chlorite reflects the intense proximal alteration and forms a distinct envelope around the orebodies (Fig. 1.3). The more intensely altered zones exhibit a near-complete replacement of the rocks by chlorite (Fig. 1.4a). Each lens displays its own conformable alteration halo in chlorite, with no connection to the neighbour orebodies. The Watson rhyolite contains poor mineralization outside these zones of intense alteration. Talc is present in variable proportions throughout the deposit and is particularly abundant in the Perseverance-West alteration halo. The mineral is closely associated with chlorite (Fig. 1.4f) and represents intense proximal alteration; chlorite and talc are both affected by the schistosity. In proximity to the orebodies, the volcanic rocks are also commonly replaced by a patchy silicification (Fig. 1.4g). This silicification is particularly intense within the Key Tuffite unit and appears to have migrated in a pervasive fashion while highlighting the primary bedding. Another generation of fine-grained white quartz fills the amygdules of the different units and underlines the

primary spherulitic crystallization textures.

Unlike many VMS systems, the hanging wall of the Perseverance deposit exhibits intense hydrothermal alteration, dominated by magnesium-rich chlorite. In the Dumagami rhyodacite, chlorite alteration varies from pervasive, with a near-complete replacement of the rocks (Fig. 1.4a), to patchy throughout the unit (see also Alteration Geochemistry below). Chlorite grains within the patchy alteration facies show combined recrystallization and realignment parallel to the planes of foliation (Fig. 1.4h).

1.4.4 Metal zonations

Metal zonations of the Perseverance orebodies are illustrated in Figure 1.5 on the basis of the geological boundaries used in Figure 1.3. These sections cut the thickest zones of the Equinox and Perseverance-West orebodies and are considered to be representative of the metal distributions at Perseverance. Copper and zinc sections constructed for Equinox and Perseverance-West (Fig. 1.5a and b) are based on blocks of 2.5 m-side with a thickness of one block and display distinct mineral zonations. Sections in zinc (Fig. 1.5a) show trends of increasing grades toward the upper portion of the orebodies, as observed for Equinox, where highest grades (reaching 38.7 wt% Zn) are located below the hanging wall contact. Similar trend is apparent at Perseverance-West, where highest grades (reaching 37 wt% Zn) are located within the upper half portion of the lens with a more peripheral attitude. The section in copper for Equinox (Fig. 1.5b) shows a slight trend of increasing grades toward the upper portion of the lens (reaching 3.1 wt% Cu). Similar variations are more pronounced in Perseverance-West with increasing copper grades toward the upper - and peripheral - portion of the orebody (reaching 4.7 wt% Cu). Both orebodies are globally poor in copper toward their lower portions (below 230 m for Equinox and 155 m for Perseverance-West).

1.5 Alteration Geochemistry

The analysis of alteration zones associated with VMS deposits provides valuable information into the processes that controlled their formation and location (Riverin and Hodgson, 1980; Gemmell and Fulton, 2001; Gemmell and Herrmann, 2001; Franklin et al., 2005). In contrast to footwall alteration zones, the recognition of hanging-wall alteration is more difficult, as the mineralogical, compositional, and textural changes are commonly less pronounced (Doyle and Allen, 2003; Franklin et al., 2005). In this section, the whole-rock compositions of both the footwall and hanging-wall zones will be used to establish their relationship to the genesis of the massive sulfide orebodies.

1.5.1 Lithogeochemistry

The volcanic and intrusive rocks of the Perseverance area are plotted in a TiO_2 vs. Zr diagram (Fig. 1.6a), to determine their magmatic fractionation trends and alteration patterns. These two elements are used for their behavior to remain immobile during hydrothermal alteration and metamorphism (MacLean and Kranidiotis, 1987; MacLean, 1990). The diagram shows linear trends with high correlation and positive slopes for all lithologies, confirming the immobility of those elements. TiO_2 and Zr are continuously enriched over the compositional range due to their incompatibility and illustrate igneous fractionation at Perseverance. During hydrothermal alteration, mass changes of mobile components cause changes in the concentration of immobile elements. This generates a spread of data along the linear trend (Fig. 1.6a) with net mass gains moving the rocks toward the origin, while net mass loss move compositions in the opposite direction (MacLean and Barrett, 1993).

Both the footwall Watson rhyolite and hanging-wall Dumagami rhyodacite are associated to low TiO_2/Zr ratios and their spread of data illustrates significant

internal mass changes. Data further indicate a clear independent pattern between the Watson rhyolite and the Dumagami rhyodacite, which reinforces the established lithostratigraphy in the vicinity of the Perseverance deposit.

1.5.2 Alteration indexes

Two alteration indexes have been tested on the footwall and hanging wall geochemical data sets (Fig. 1.6b). The alteration index (AI: Ishikawa et al., 1976) relates to the replacement of plagioclase by sericite and chlorite during hydrothermal alteration, while the chlorite-carbonate-pyrite index (CCPI: Large et al., 2001) measures the degree of chlorite, pyrite and/or carbonate alteration. Large proportions of the AI and CCPI values plot well outside the 'least altered' box, indicating significant geochemical changes during hydrothermal alteration for both the footwall and hanging wall trends. Alteration index values range from 14.1 to 99.1 and CCPI index values vary from 29.8 to 99.9 for the hanging wall Dumagami rhyodacite. Sharp geochemical changes are associated with a marked trend in chlorite-pyrite, which dominates the AI-CCPI box plot. Other alteration trends in sericite, epidote, carbonate and K-feldspar are not marked or are absent in the immediate vicinity of the deposit.

1.5.3 Precursor selection and mass balance calculations

An evaluation of the mass changes undergone by mobile elements during hydrothermal alteration was made in Perseverance using the equation of Gresens (1967), further adapted by Grant (1986, 2005). Absolute mass gains and losses were calculated in the footwall and hanging wall rocks with respect to a composite single precursor composition selected for each unit and compared to all other samples (see calculation details in Methodology). Composite precursors were selected in the least

altered box of the two alteration indexes diagram: a group of three precursors was selected for comparison with 1066 whole rock analyses of Watson rhyolite and a group of two samples was selected for comparison with 645 analyses of Dumagami rhyodacite. Least altered samples were also chosen from drill holes intersecting the volcanic rocks tens to hundreds of meters away from the proximate alteration plume of the orebodies and show no visible effect (hand sample and thin section observations) of hydrothermal alteration. Geochemical compositions for the footwall rhyolite and the hanging wall rhyodacite with their respective precursor compositions are listed in Table 1.

1.5.4 Mapping of mass balance results

A representation of the mass changes at Perseverance allows identifying the zones affected by hydrothermal alteration in the host volcanic rocks and their geometric relationships with the massive sulfide orebodies. Mass balance results are represented in two plans corresponding to the Watson rhyolite and Dumagami rhyodacite in accord with the subhorizontal stratigraphy of the units at Perseverance. The two plans have vertical thicknesses of 170 m for the Watson rhyolite, 80 m for the Dumagami rhyodacite and such representation implies a projection of the sample positions at the same level that the ore contours (from below in the footwall and from above in the hanging wall). Repartitions of whole rock analysis used for mass balance calculations relative to the location of the orebodies are given in Figures 1.7a and b, whereas Figures 1.7c to h show corresponding mass changes (in wt%) for representative major mobile elements.

Mass balance calculations reveal significant variations in the footwall and hanging wall rocks for the major elements MgO, K₂O and Na₂O. Mapping of MgO in the footwall Watson rhyolite (Fig. 1.7c) underlines sharp absolute mass gains with values exceeding 10 wt% (highest value reaches 49 wt%). These mass gains form

large halos closely correlated with the location of the four orebodies. Mass balance results also reveal strong absolute mass gains of MgO in the hanging wall Dumagami rhyodacite (Fig. 1.7d), with values that similarly exceed 10 wt% (highest value reaches 17 wt%). Although less developed than in the footwall, the halos corresponding to mass gains are particularly correlated with the location of the orebodies, as observed at Perseverance-Main/Perseverance-2 and Perseverance-West. Geochemical data show that persistent mass gains of MgO can be traced for up to 70 m above the orebodies in the hanging wall Dumagami rhyodacite. Drillcore observations and detailed mapping of the volcanic host rocks at Perseverance indicate that the geochemical anomalies of MgO correspond to the presence of black magnesian chlorite. This is also confirmed by the main trend of the alteration box plot in Figure 1.6b. MgO values can also reflect variable amounts of talc, as this mineral is locally abundant in the Perseverance alteration assemblage (Fig. 1.4f).

Mass balance calculations for the alkali components K₂O and Na₂O are also relevant at Perseverance. Mapping of K₂O in the footwall Watson rhyolite (Fig. 1.7e) underlines significant absolute mass losses with lowest values reaching -2.1 wt%. These mass losses form large halos closely correlated with the location of the four orebodies. Mass balance results also reveal strong absolute mass losses of K₂O in the hanging wall Dumagami rhyodacite (Fig. 1.7f), with values in the order of -1 wt% (lowest value at -1.2 wt%). Although, the halos associated to K₂O mass losses are less developed than in the footwall, they are particularly correlated with the location of the orebodies. It is further interesting to notice that halos shapes corresponding to K₂O mass losses match perfectly those of MgO mass gains in both the footwall and hanging wall rocks. In correlation with K₂O, mapping of Na₂O also underlines significant absolute mass losses in the footwall (Fig. 1.7g) with values reaching -4 wt% and in the hanging wall (Fig. 1.7h) with similar depletions. Mass losses in Na₂O are globally correlated with the location of the orebodies and are still significant (in the order of -3 wt%) when moving away from them in the deposit.

In comparison to large enrichments of MgO in the volcanic sequence, the values associated to depletions in alkali components are considered relevant when taking into account the low initial concentrations of the corresponding precursors before hydrothermal alteration (see also Table 1.1). Petrographic evidences indicate that K₂O and Na₂O mass losses result directly from the breakdown of feldspar during chloritization. Plotting of MgO versus K₂O compositions generate a negatively correlated trend, which sustains the link between chloritization and depletion in alkalis.

1.6 Structural Geology

The Perseverance deposit shows a variety of deformation features recorded in both the orebodies and the immediate host rocks. Structural modifications are present at different scales of observation, and have resulted in significant changes of the original setting.

1.6.1 Host-rock setting

The south flank of the district has historically been described as weakly affected by the deformation, or where present, to be confined to narrow brittle-ductile shear zones (Piché et al., 1993; Lavallière et al., 1994). In the vicinity of Perseverance, a series of outcrops corresponding to the footwall Watson rhyolite, display a penetrative schistosity. The fabric dips vertically and crosscuts all primary flow structures of the Watson rhyolite. This schistosity is particularly well developed in the immediate envelope of the ore zones, where hydrothermal alteration is pronounced. Schistosity measurements were taken in the host rocks of the Perseverance deposit and data yield an average plane oriented at N105° with near vertical plunges (Fig. 1.8a). This global northwest-southeast direction corresponds to

the orientation of S_1 , associated with the regional deformation stage D_1 . Mineral stretching lineations L_1 observed within the northwest-southeast foliation planes have a moderate to steep plunge to the west (Fig. 1.8a).

Original bedding (S_0) of the volcanic sequence around the deposit is indicated by the depositional laminations of the Key Tuffite unit. Drill holes in the south flank indicate that this unit lies along a uniform plane dipping to the northwest, with a value of $\sim 20^\circ$ around Perseverance (Arnold, 2006). In the immediate vicinity of the deposit and within a radius of <100 m from the orebodies, the Key Tuffite displays steeper dips and is affected by numerous folds. These folds are generally of metric scale, ranging from open to isoclinal and the measurement of related S_0 attitudes shows that their average axial plane, F_{KT} , parallels the regional schistosity S_1 at N110° (Fig. 1.8a, b). The Key Tuffite is also deformed into larger folds at the scale of the orebodies, as in Perseverance-West where a >100 m wide antiform structure envelops the orebody (Fig. 1.3b); diamond drill hole information indicates that this fold is non-cylindrical. Based on underground observations, folding in the Key Tuffite increases in intensity in the zones where chlorite alteration is recorded, suggesting a spatial correlation (Fig. 1.9a).

A systematic orientation of the orebodies can be highlighted on a map showing their projection to the surface (Fig. 1.2). The lenses Equinox, Perseverance-Main and Perseverance-2 have an oblate shape parallel to a northwest-southeast direction. In projection, the individual sulfide lenses have variable strike extents along their major axes: 175 m at Equinox, 135 m at Perseverance-Main, 80 m at Perseverance-West and 50 m at Perseverance-2. Thickness of the ore at Equinox varies from several meters to ~ 110 m (Fig. 1.2, 1.3a). The shape of the Perseverance-West lens is more irregular, but displays two branches at its northern and southern extremities that follow a northwest-southeast trend (Fig. 1.3b). The global northwest-southeast elongation pointed out in the Perseverance orebodies corresponds to the direction of the regional schistosity S_1 at N105°. The four lenses also mark a

moderate to steep plunge towards the northwest, thus displaying an attitude globally similar to that of the mineral stretching lineations recorded in volcanic host-rocks (Fig. 1.8).

1.6.2 Massive sulfide structures

Distinct mineralogical banding is developed in the four massive sulfide orebodies of Perseverance, characterized by millimeter- to centimeter-thick monomineral bands of pyrite alternating with sphalerite as well as lesser amounts of pyrrhotite, chalcopyrite and magnetite (Fig. 1.4c). The mineralogical banding represents a dominant texture in the ore and was recognized at all stratigraphic levels of the lenses, from their base to the hanging wall contact. It was also noticed that the ribbon-texture is usually better developed in zinc-rich zones where the massive pyrite ore is less abundant. Sulfide minerals are generally associated with small amounts of gangue minerals such as quartz and chlorite with subordinate talc, actinolite and calcite. Mineral assemblages involved in the ribbon-texture are generally finer-grained than in the other facies.

In Perseverance, the planes formed by this mineralogical banding are essentially vertical and therefore clearly discordant to the subhorizontal volcanic sequence that hosts the deposit. The attitudes corresponding to the planes of banding were measured in the Equinox, Perseverance-West and Perseverance-Main orebodies and recorded in stereograms (Fig. 1.8). The average banding directions are identical for Equinox and Perseverance-Main and give a general northwest-southeast orientation at N110° with minor changes around a subvertical dip (Fig 1.8c, d). This direction matches closely the attitude of the regional schistosity S_1 for the Equinox and Perseverance-Main orebodies and with less correlation for Perseverance-West. The global banding direction at Perseverance-West shows a deviation towards the northeast with an average plane at N80° (Fig 1.8e). A possible relation can be pointed

out between this direction and the S_2 schistosity developed in the north flank of the district at $\sim N75^\circ$.

In the massive sulfide orebodies, the ribbon-textured ore is associated to ovoidal-elongate structures that parallel and interrupt the banding. These centimeter-to meter-wide structures are composed of fragments ranging from single crystals to large blocks (Fig. 1.9b). Fragments are typically angular to rounded, and show evidence of internal rotations. The brecciated rock is generally composed of pyrite and magnetite with variable proportions of silicate material including altered rhyolite, while the matrix of banded-ore usually contains sphalerite, chalcopyrite and pyrrhotite mixed with pyrite. Vokes (1973) and Marshall and Gilligan (1989) introduced the German term "durchbewegung" to describe deformation in which internal rotational movements dominate. Durchbewegung structures characterize rotations of relatively competent ore materials in a matrix of predominantly incompetent material during deformation. Common sulfides - except pyrite - usually behave in a more ductile fashion than most silicate rocks throughout regional metamorphism (Marshall and Gilligan, 1987). A rheology contrast is illustrated at Perseverance between assemblages formed by typically strong materials (pyrite, magnetite and silicate rocks) and a matrix of relatively weaker sulfides (sphalerite, chalcopyrite and pyrrhotite) characterizing the banded ore. Associated disorientations and deformations characterize the formation of durchbewegung structures. Roberts (1975) and Piché et al. (1993) described the presence of singular mineral assemblages in the orebodies of the Matagami Lake and Norita mines that present strong similarities with these deformation-related structures.

Among the different generations of intrusions, tholeiitic gabbros constitute the most represented network of dikes within the ore at Perseverance. The gabbro dikes present in the orebodies are rarely continuous and are associated to numerous evidences of deformation. They are either affected by folding, boudinage or by a combination of both. Folding is generally displayed in centimeter- to meter-thick

dikes that crosscut the ore at subhorizontal attitudes. These folds are generally tight to isoclinal and display an apparent shortening of 40% when present in the massive sulfides (Fig. 1.9c).

Deformation by boudinage affects a large number of gabbro dikes present in the massive sulfides regardless their thickness. Dikes are characterized by variable orientations and the development of boudins is maximal for subvertical attitudes (Fig. 1.9d, e). Elongation of the boudins systematically parallels the planes of banding where a ribbon texture constitutes the matrix to the dikes. Observations of the dike geometries in three dimensions indicate that boudin necks are oriented both towards the *X*- and *Y*-directions within the planes of banding, thus indicating stretching in two directions. Boudins generally form where competent layers are extended into pieces by a contrast of viscosity with a rock matrix that deforms plastically. The presence of boudinaged dikes in massive sulfides indicates differences of competence between the materials during deformation. Varying shapes of the boudins (rounded to rectangular) also show that the type of ore (banded pyrite-sphalerite to massive pyrite) induces contrasts of competence with a similar gabbroic material during the deformation.

Separations between boudins are commonly associated with passive folding in the massive sulfides. At the interface between materials of different competency, the massive sulfides also form transgressive vein-like bodies that consistently extend into the more competent silicate material. At Perseverance, such structures are commonly developed at the contact between massive sulfides and various lithologies including dikes, rhyolites and the Key Tuffite (Fig. 1.9f). These centimeter- to meter-long penetrative structures, termed piercement veins are common in the Perseverance deposit and constitute a characteristic deformation feature of massive ores (Gilligan and Marshall, 1987; Duuring et al., 2007). Piercement veins reflect layer-parallel or layer-oblique (shallow-angle) contraction of an interface separating materials with contrasts of competency. The structures develop due to layer-parallel delamination in

the competent material, where withdrawal of incompetent material becomes more difficult than penetrating competent rock (Marshall and Gilligan, 1989). Where observed within the ribbon-textured ore in Perseverance, piercement veins have an orientation normal to the planes of banding.

1.6.3 Mineral fabrics

Both banded ore and massive pyrite ore typically consist of granoblastic, fine-grained pyrite crystals with anhedral to subhedral textures (Fig. 1.9g). Pyrite grains are locally coarser and also occur as large (up to 3 cm) porphyroblasts. In the banded ore, coarse pyrite grains are commonly flattened and display elongations parallel or subparallel to the mineralogical banding. In parts of the ore where other sulfides are less abundant, pyrite grains show straight or gently curved boundaries and characteristic equilibrium triple junctions at grains boundaries (Fig. 1.9g). The development of roughly equant grains with 120° dihedral angles, referenced to as 'foam' texture, is indicator of metamorphic recrystallization through annealing (Vokes and Craig, 1993; Craig et al., 1998). Individual metablasts and pyrite-rich aggregates are also commonly affected by intense brittle deformation and broken by conjugate fractures (Fig. 1.9h). Subhedral magnetite grains in the ores are commonly undeformed and display the same behavior than pyrite grains, indicating that they acted as high-strength inclusions in weaker and more ductile matrix sulfides.

Pyrite triple junction boundaries, together with the fractures developed in coarse pyrite grains, are commonly infilled with matrix sulfides of the polymetallic assemblage (Fig. 1.9h). In zones with higher matrix sulfides to pyrite ratios, chalcopyrite shows a textural evidence of remobilization by creeping in metablastic pyrite grains, sometimes in association with sphalerite (Fig. 1.9h). In the ore, chalcopyrite aggregates are commonly organized under the form of pressure shadows at the extremities of silicate inclusions, pyrite and/or magnetite grains, (Fig. 1.9e).

Where present in the banded ore, the chalcopyrite also systematically parallels the banding formed by pyrite and sphalerite in the direction of stretching lineation. This behavior of chalcopyrite (\pm sphalerite) at microscopic scale is analogous to observations made at larger scales in the orebodies. Where small centimeter-scale folds are observed in the ore, the chalcopyrite is systematically enriched relative to pyrite and sphalerite in hinge zones. Although it is difficult to estimate the maximum distance associated with the creeping of chalcopyrite during deformation, it is clear that this phenomenon is not limited to crystal scale but rather could cover several tens of centimeters or more. The systematic structural behavior of chalcopyrite (\pm sphalerite) relative to more competent minerals/clasts highlights the record of a spatial reorganization in response of ductility contrasts at Perseverance.

Disseminated ores in volcanic host rocks generally show much less internal evidence of deformation, although sulfide aggregates commonly exhibit elongation parallel to the main foliation. Disseminated ores also display strong physical retexturing by the metamorphic intergrowth of sulfide and gangue minerals.

1.7 Discussion

1.7.1 Evidence for subseafloor replacement

VMS deposits of the Matagami district are often cited as classical examples of exhalative-style mineralization (Piché et al., 1993; Ioannou and Spooner, 2007; Ross et al., 2014). Close spatial relationships in the volcanic sequence between the regional Key Tuffite stratigraphic marker and most of the massive sulfide deposits have long time suggested a genetic connexion in favor to seafloor ore deposition (Roberts, 1975; Davidson 1977; Liaghat and Maclean, 1992; Lavallière et al., 1994). In an uncommon stratigraphic setting for the Matagami district, the Perseverance deposit contains a series of evidences suggesting a formation by subseafloor replacement.

Significant portions of massive sulfides of the deposit crosscut the Key Tuffite unit over several tens of meters and are in direct contact with the hanging wall Dumagami rhyodacite. Stratigraphic relationships of the Key Tuffite in the vicinity of the orebodies indicate that this framework corresponds to original ore boundaries, despite the presence of a post-volcanic deformation overprint (see below). The ubiquitous presence of volcanic clasts in the orebodies, with textures and alteration identical to that of the surrounding host rocks, is also diagnostic for a replacement front beyond the footwall Watson rhyolite. Only sporadic relicts of the Key Tuffite were identified within the sulfides at Perseverance due to the presence of intense chloritization, but their presence is clearly attested at the Isle Dieu deposit (Lavallière et al., 1994). Genna et al. (2014) showed that the alteration recorded in the Key Tuffite unit is largely epigenetic in style and forms a coherent pattern proximal to the deposits. In particular, they documented that a mineral assemblage composed of chlorite, silica and sulfides formed from selective replacement of the primary layering as a function of grain size and therefore primary porosity of the rock. The nature of the Key Tuffite unit is reinterpreted to be dominated by andesitic ash with a negligible or absent exhalative component. The lack of genetic connexion between massive sulfides and the Key Tuffite unit allows alternative scenarios of ore-forming processes besides the seafloor exhalative-style model.

Seafloor VMS deposits are characterized by the development of asymmetric alteration patterns in their host volcanic sequence, with intense hydrothermal alteration in the footwall and generally weak alteration in the hanging wall (e.g., Corbet: Barrett et al., 1993; Millenbach: Knuckey et al., 1982; Gibson and Watkinson, 1990; Norbec: Shriver and MacLean, 1993). This pattern indicates that the main stage of ore-forming hydrothermal activity occurred after emplacement of the footwall rocks and before deposition of the hanging wall rocks. At Perseverance, mass balance calculations indicate a pattern of intense hydrothermal alteration in hanging wall rocks, with very little quantitative and spatial change to that present in

the footwall (Fig. 1.11a). In particular, there is strong MgO enrichment and high alteration index values, accompanied by significant depletions in K₂O and Na₂O up to 70 m above the orebodies in the Dumagami rhyodacite. In the Matagami deposits, chlorite and talc are interpreted to be contemporaneous within the proximal Mg-rich alteration assemblage (Costa et al., 1983; Galley et al., 2007). The close relationship evidenced at Perseverance between the zones of magnesium enrichment and those of depletion in alkalis is indicative of feldspars breakdown during chloritization, a common feature also described in tasmanian deposits (Gemmell and Fulton, 2001). The development of strong alteration in both the footwall and hanging wall rocks at Perseverance indicates either that an anomalously high declining hydrothermal activity continued during deposition of the hanging wall succession or that massive sulfide deposition was dominantly epigenetic in space and occurred entirely as subseafloor replacement.

Dating of the footwall Waston rhyolite and hanging wall Dumagami rhyodacite at 2725.9 ± 0.8 Ma_{U-Pb} and 2725.4 ± 0.7 Ma_{U-Pb} respectively (Ross et al., 2014) indicate, within analytical error, that they are contemporaneous. Although the rate of emplacement of the volcanic succession at Perseverance cannot be determined, the coherent facies of rhyolitic and rhyodacitic lavas are consistent with rapid emplacement as lava flows or lava domes during active volcanic construction (Allen, 1992; Galley et al., 1995; Doyle and Allen, 2003). Massive sulfides that are hosted within rapidly emplaced sedimentary or volcanic facies are more likely to form by replacement (Allen, 1995; Allen et al., 1996).

Doyle and Allen (2003) proposed five criteria that are indicative of subseafloor replacement in VMS deposits: (1) enclosure of mineralized horizons by rapidly emplaced volcanic or sedimentary facies, (2) relicts of host facies within the mineral deposit, (3) replacement fronts between the deposit and host lithofacies, (4) discordance of the deposit to bedding, and (5) strong hanging wall alteration without an abrupt break in intensity. Criterias 1, 2, 4 and 5 are documented in the

Perseverance deposit. For criteria 3, sharp replacement fronts of massive sulfides above the Key Tuffite most probably reflect an original discordant relationship, but the post-volcanic deformations recorded in the deposit (see below) may also be responsible of this setting.

Formation of the Perseverance deposit was likely related to permeability contrasts in the volcanic sequence between the relatively impermeable hanging wall Dumagami rhyodacite and favourable zones in the footwall, including the structural porosity of syn-volcanic fractures as well as primary porosities of the Watson rhyolite hyaloclastic top and of the Key Tuffite. The four orebodies present in the deposit also suggest that different permeable zones existed in the footwall volcanioclastic rocks, that promoted the deposition of multiple mineralized zones in a subseafloor setting (Fig. 1.11a).

Formation of the Perseverance deposit was likely related to favourable zones of higher permeability in the footwall, including the hyaloclastic top of the Watson rhyolite as well as the porous Key Tuffite unit and probably most importantly, the structural porosity of syn-volcanic fractures. The presence of four orebodies in the deposit also suggest that different permeable zones existed in the footwall rocks, which promoted the deposition of multiple mineralized zones in a subseafloor setting (Fig. 1.11a). It is also probable that the relatively impermeable hanging wall Dumagami rhyodacite as well as early stages of alteration/sealing of the porous Key Tuffite unit played a role in focusing the hydrothermal fluids in the volcanic sequence.

1.7.2 Post-volcanic deformation overprint

Multi-scale observations of structural and textural features in the Perseverance deposit indicate that a significant post-volcanic deformational overprint was recorded

in the massive sulfide orebodies, in relation with regional greenschist facies metamorphism.

Microscopic-scale observations on the physical behavior of the mineral assemblage give a good indication of the degree of deformation and related processes that were imprinted on the Perseverance deposit during regional metamorphism. In the orebodies, evident contrasts of strength behavior can be pointed out: pyrite and magnetite show evidence of brittle deformation, whereas chalcopyrite appears to have deformed in a ductile manner over most of the deformation history. Sphalerite has a transitional behavior with favourable ductile-style deformation and commonly displays strong annealing.

Many workers documented the mechanical behavior of common minerals in massive sulfide deposits through experimental work for varying conditions of temperature, pressure, stress-differential and strain-rate (Clark and Kelly, 1976; Cox, 1987; Marshall and Gilligan, 1987). Most of the sulfides (galena, chalcopyrite, pyrrhotite and sphalerite, but not pyrite), are variably affected by cataclasis or dislocation flow at metamorphic temperatures, and exhibit dynamic recrystallization under low-grade metamorphic conditions (Marshall and Gilligan, 1993). Chalcopyrite and pyrrhotite behave in a ductile manner at least down to 200°C and 250 °C respectively, with strength and deformation mechanisms dependent on temperature; and at low temperature-pressure conditions, dependent on confining pressure (Fig. 1.10) (Clark and Kelly, 1976; Marshall and Gilligan, 1993). Pyrite and magnetite are much less ductile than the other sulfides over a wide temperature-pressure range (Fig. 1.10). At low temperature, pyrite has been found to deform by brittle fracture (Craig et al., 1998); however, above 400°C it can deform by dislocation processes (Cox et al., 1981). McClay and Ellis (1983) have shown that at low-temperature (<300°C), pressure solution and cataclasis are the major pyrite deformation mechanisms. At Perseverance, for temperatures corresponding to greenschist facies in the range of

300°C - 400°C, solid-state mechanical transfers related to ductile behavior represent the dominant deformation mechanism in sulfides (Fig. 1.10).

VMS deposits commonly display temperature zonations resulting in the distribution of copper from chalcopyrite at the base and within the core of the deposits (Lydon, 1984; Galley et al., 2007). Metal distributions in the Perseverance orebodies contrast with this setting as highest copper grades are widely scattered throughout the orebodies and tend to be located at their upper extremities (e.g., Equinox) or in peripheral zones (e.g., Perseverance-West). Field and experimental data (Fig. 1.10) show that chalcopyrite constitutes one of the less competent minerals of the polymetallic assemblage and show evidence for ductile behavior with respect to local conditions of metamorphism. The contrast of competence (or viscosity) of chalcopyrite allows a mechanical remobilization of copper with its most effective window typically occurring in the approximate range of 250°C - 500°C, in association with a scale of diffusion of tens to less than 100 m (Marshall and Gilligan, 1993). Field observations on dikes present within the ore show that important strain values - in the order of 40% - are reached in the massive sulfide orebodies of Perseverance. These data indicate that steady state flow was attained, thus allowing the diffusion of elements over time (Cox, 1987). The ductile behavior of chalcopyrite, together with these observations, suggest that the chalcopyrite distribution of the Perseverance orebodies is related to the post-volcanic deformation overprint, and obliterates the original syn-volcanic pattern (Fig. 1.11b). Remobilization is here interpreted to be internal to the orebodies and did not generate external and transposed oreshoots.

The sulfide banding developed along vertical attitudes at Perseverance is discordant to the subhorizontal volcanic sequence, thus contrasting with concordant primary bedding associated with seafloor-style massive sulfide deposits (Galley et al., 2007). Previous workers pointed out the presence of a mineralogical banding in several massive sulfide deposits of the Matagami district (Sharpe, 1968; Roberts, 1975; Lavallière et al., 1994; Piché et al., 1993). At Isle-Dieu, Lavallière et al. (1994)

also observed discordant relationships between a vertical banding in the sulfides and the host lithologies. This was then interpreted as a syn-volcanic texture resulting from a particularly evolved stockwork system, i.e. «atypical massive sulfide chimneys». At Perseverance, the attitude of mineralogical banding developed within the Equinox and Perseverance-Main orebodies (i.e. N 110°), is remarkably parallel to the regional schistosity S_1 of the surrounding volcanic host rocks (i.e. N 105°) as well as the folding directions of the Key Tuffite (i.e. axial plane at N 110°). Orientations of the mineralogical banding at Perseverance-West (i.e. N80°) can possibly be related with the S_2 schistosity developed in the north flank of the district. At the microscopic scale, many deformation and recrystallization textures, including the ductile behavior of chalcopyrite, total annealing of sphalerite and reorientation of pyrite grains along favourable planes, clearly show that the mineralogical banding is a texture associated to the post-volcanic deformation overprint (Fig. 1.11b). These observations indicate the transposition of sulfide minerals subparallel to the main foliation, as documented elsewhere in Abitibi (e.g., LaRonde: Dubé et al., 2007). The development of a mineral banding in the Perseverance orebodies at greenschist facies can be explained by two types of deformation processes. On one hand, the banding is interpreted as a metamorphic fabric formed during exsolution of low-temperature sulfides from deforming medium- to high-temperature phases such as monosulfide solid solution (McQueen, 1987). On the other hand, the banding could be the result of mechanical segregation of separate sulfides during ductile deformation (McDonald, 1970; Cowden and Archibald, 1987). At Perseverance, evidence against layer formation by purely mechanical means include the diffuse and anastomosing nature of some layers and the concentration of both weak and competent minerals together in the same layer (e.g. pyrite-chalcopyrite, pyrite-sphalerite and pyrrhotite-chalcopyrite). Mechanical segregation in polymimetic aggregates would tend to produce monomineralic layers of minerals with different strength characteristics and deformation behavior. Band formation depends on the degree to which the sulfides were homogenized during

metamorphism. It is suggested for Perseverance that both mechanical and exsolution band-forming processes operated and that a complex interplay existed between dissolution, exsolution, and mechanical segregation during metamorphism.

The massive sulfide orebodies of Perseverance are characterized by atypical elongated geometries, with global flattening parallel to the main foliation S_1 . Mineral stretching lineations also appear to have an effect on the orebodies along westerly plunges. Oreshoots paralleling the elongation direction are very common in deformed rocks (Lacroix et al., 1993; Marshall and Gilligan, 1993; Mercier-Langevin et al., 2013). At Perseverance, the development of a high degree of recrystallization and remobilization in the ore contrasts with the relatively low deformation observed in the south flank volcanic rocks outside narrow corridors of deformation. Common sulfides, except pyrite, have much lower effective viscosities than silicate rocks throughout the global range of regional metamorphism (McClay and Ellis, 1983; Marshall and Gilligan, 1987). The pronounced contrast of rheology between ductile sulfides of the polymetallic assemblage and more competent silicate host rocks (rhyolites and rhyodacites) will favor strain accommodation in the orebodies. Similar discontinuities occur at smaller scale within the sulfide assemblage for the formation of durchbewegung structures, piercement veins and boudinaged dikes. In contrast to its accompanying sulfides which often undergo ductile deformation, pyrite is much more refractory to the stress and retains many characteristics, even in deposits subject to penetrative deformation (Cox, 1987; Craig et al., 1998).

The Perseverance orebodies are exceptionnaly rich in zinc with 5.2 Mt at 15.8 wt% Zn and significant portions of ore exceed 30 wt% Zn. They consequently contain lesser proportions of pyrite and it is suggested that the relatively high degree of deformation accomodated at Perseverance is intimately connected to this primary compositional setting. Secondary morphologies imprinted on the Perseverance orebodies challenge the understanding of their original geometries related to the syn-volcanic environment. Based on field observations, remobilization of sulfides

external to the orebodies during deformation appears limited and the presence of massive sulfides in direct contact with the Dumagami rhyodacite at the hanging wall reflects an original pattern of deposition by subseafloor replacement (Fig. 1.11a). Independent alteration halos around the lenses (cf. Alteration Geochemistry) also suggest that no major dismemberment occurred during deformation and that the presence of four massive sulfide orebodies is an original characteristic. In the vicinity of the Perseverance deposit, chlorite alteration zones around the massive sulfide orebodies are strongly affected by the schistosity and field observations indicate that they can be correlated with the zones where folds are developed in the Key Tuffite. It is evident that the contrast of competence between hydrothermally chloritized (lower viscosity) and relatively fresh volcanic host rocks (higher viscosity) together with the presence of a mass of sulfides, has exerted an effect on fold localization.

1.8 Conclusion

Four vertical pipelike massive sulfide bodies characterize the Perseverance deposit with a perpendicular attitude to the local low dipping (20° NW) volcanic sequence. Style and setting of the Perseverance deposit bring new insights into the mechanisms of formation of VMS deposits at Matagami and point out the presence of significant subsequent modifications over the volcanic framework in the south flank of the district.

The Perseverance deposit is interpreted to have formed as subseafloor replacement, through the support of: 1) discordant relationship between the ore envelopes and bedding, 2) presence of hanging wall relicts within the ore, 3) intense pervasive alteration into the hanging wall, and 4) evidence for rapid volcanic emplacement. Genesis of the four lenses was likely related to permeability contrasts in the volcanic sequence and controlled by primary and structural porosities of specific zones within the units. This syn-volcanic framework was overprinted by an

intense deformation during regional greenschist facies metamorphism. The deformation is controlled by competency contrasts related to varying material ductility in the polymetallic sulfide assemblage and against silicate host rocks. In addition to sharp modifications of the global geometries, many textures and structures reflect the deformation and include a vertical mineral banding, strong boudinage, folding, as well as durchbewegung and piercement structures. Chalcopyrite displays evidence for remobilization and suggests that original copper zonations were significantly modified during metamorphism.

Several elements documented at Perseverance provide useful guidelines for future VMS exploration strategies in the district and in other similar environments. Pervasive hanging wall alteration is recognized as one of the processes associated with ore deposition. Consequently, magnesium enrichments combined with depletions in alkali elements should be carefully examined in the hanging walls of the targets, especially in areas of low to moderate dips. Additionally, chlorite alteration zones have accommodated most of the post-ore strain due to their ductility. Consequently, hydrothermal alteration halos are spatially correlated with the deformation zones despite the lack of a genetic relationship. Recognition of ductile deformation in fertile volcanic rocks - such as folds in the Key Tuffite - in relation with alteration zones would aid exploration success.

Acknowledgments

This paper form parts of a M.Sc. thesis by the first author. Glencore Canada Corporation (formerly Xstrata Zinc), Donner Metals, Mitacs Acceleration, Consorem and Divex are thanked for financing this study. We are grateful for numerous discussions with Glencore production and exploration geologists, including R. Dussault, J. Drapeau, R. Nieminen, R. Brassard and M. Dessureault, who helped in the work undertaken at the Perseverance mine and for access to unpublished data.

The study has benefited from the scientific contribution of M. Gauthier who is thanked for constructive discussions in the field. An early version of the manuscript greatly benefited from the review of J. Franklin, J. Hedenquist and A. Tremblay. M. Laithier is thanked for her contribution in the preparation of the figures.

References

- Adair, R. 2009, Technical report on the resource calculation for the Bracemac-McLeod discoveries, Matagami, Quebec: National Instrument 43-101, Donner Metals Ltd., 194 p. <http://www.sedar.com>. Accessed 11 Dec 2014
- Adam, E., Milkereit, B., Mareschal, M., 1998. Seismic reflection and borehole geophysical investigations in the Matagami mining camp. Canadian Journal of Earth Sciences 35, 686–695.
- Allen, R., 1995, Synvolcanic, subseafloor replacement model for Rosebery and other massive sulphide ores: Geological Society of Australia Abstracts, 1995, p. 107-108.
- Allen, R. L., 1992, Reconstruction of the tectonic, volcanic, and sedimentary setting of strongly deformed Zn-Cu massive sulfide deposits at Benambra, Victoria: Economic Geology, v. 87, p. 825-854.
- Allen, R. L., Weihsed, P., and Svenson, S.-A., 1996, Setting of Zn-Cu-Au-Ag massive sulfide deposits in the evolution and facies architecture of a 1.9 Ga marine volcanic arc, Skellefte district, Sweden: Economic Geology, v. 91, p. 1022-1053.
- Arnold, G., 2006, Feasibility study update of the Perseverance project, Matagami, Quebec: Falconbridge Limited, 178 p.
- Barrett, T., MacLean, W., Cattalani, S., and Hoy, L., 1993, Massive sulfide deposits of the Noranda area, Quebec. V. The Corbet mine: Canadian Journal of Earth Sciences, v. 30, p. 1934-1954.
- Beaudry, C., and Gaucher, E., 1986, Cartographie géologique dans la région de Matagami. Ministère de l'Energie et des Ressources du Québec, MB-86-32.
- Carr, P. M., Cathles, L. M., and Barrie, C. T., 2008, On the size and spacing of volcanogenic massive sulfide deposits within a district with application to the Matagami district, Quebec: Economic Geology, v. 103, p. 1395-1409.

- Clark, B., and Kelly, W., 1976, Experimental deformation of common sulphide minerals: The physics and chemistry of minerals and rocks: New York, NY, John Wiley and Sons, p. 51-70.
- Costa, U., Barnett, R., and Kerrich, R., 1983, The Mattagami Lake Mine Archean Zn-Cu sulfide deposit, Quebec; hydrothermal coprecipitation of talc and sulfides in a sea-floor brine pool; evidence from geochemistry, $\delta^{18}\text{O}/\delta^{16}\text{O}$, and mineral chemistry: Economic Geology, v. 78, p. 1144-1203.
- Cowden, A., and Archibald, N. J., 1987, Massive-sulfide fabrics at Kambalda and their relevance to the inferred stability of monosulfide solid-solution: Canadian Mineralogist, v. 25, p. 37-50.
- Cox, S., 1987, Flow mechanisms in sulphide minerals: Ore Geology Reviews, v. 2, p. 133-171.
- Cox, S., Etheridge, M., and Hobbs, B., 1981, The experimental ductile deformation of polycrystalline and single crystal pyrite: Economic Geology, v. 76, p. 2105-2117.
- Craig, J., Vokes, F., and Solberg, T., 1998, Pyrite: physical and chemical textures: Mineralium Deposita, v. 34, p. 82-101.
- Davidson, A. J., 1977, Petrography and chemistry of the key tuffite at Bell Allard, Matagami, Quebec, M. Sc. thesis, Montreal, Canada, McGill University, 153 p.
- Doyle, M. G., and Allen, R. L., 2003, Subsea-floor replacement in volcanic-hosted massive sulfide deposits: Ore Geology Reviews, v. 23, p. 183-222.
- Dubé, B., Mercier-Langevin, P., Hannington, M., Lafrance, B., Gosselin, G., and Gosselin, P., 2007, The LaRonde Penna world-class Au-rich volcanogenic massive sulfide deposit, Abitibi, Quebec: mineralogy and geochemistry of alteration and implications for genesis and exploration: Economic Geology, v. 102, p. 633-666.
- Duuring, P., Bleeker, W., and Beresford, S., 2007, Structural modification of the komatiite-associated Harmony nickel sulfide deposit, Leinster, Western Australia: Economic Geology, v. 102, p. 277-297.
- Franklin, J., Gibson, H., Jonasson, I., and Galley, A., 2005, Volcanogenic massive sulfide deposits: Economic Geology 100th anniversary volume, v. 98, p. 523-560.
- Galley, A., Watkinson, D., Jonasson, I., and Riverin, G., 1995, The subsea-floor formation of volcanic-hosted massive sulfide; evidence from the Ansil Deposit, Rouyn-Noranda, Canada: Economic Geology, v. 90, p. 2006-2017.

- Galley, A. G., Hannington, M., and Jonasson, I., 2007, Volcanogenic massive sulphide deposits: Mineral Deposits of Canada: A Synthesis of Major Deposit-Types, District Metallogeny, the Evolution of Geological Provinces, and Exploration Methods: Geological Association of Canada, Mineral Deposits Division, Special Publication, v. 5, p. 141-161.
- Gemmell, J. B., and Fulton, R., 2001, Geology, genesis, and exploration implications of the footwall and hanging-wall alteration associated with the Hellyer volcanic-hosted massive sulfide deposit, Tasmania, Australia: Economic Geology, v. 96, p. 1003-1035.
- Gemmell, J. B., and Herrmann, W., 2001, A Special Issue on Alteration Associated with Volcanic-Hosted Massive Sulfide Deposits, and Its Exploration Significance: Economic Geology, v. 96, p. 909-912.
- Genna, D., Gaboury, D., and Roy, G., 2014, The Key Tuffite, Matagami Camp, Abitibi Greenstone Belt, Canada: petrogenesis and implications for VMS formation and exploration: Mineralium Deposita, v. 49, p. 489-512.
- Gibson, H. L., and Watkinson, D., 1990, Volcanogenic massive sulphide deposits of the Noranda cauldron and shield volcano, Quebec: Canadian Institute of Mining and Metallurgy, p. 119-132.
- Gilligan, L., and Marshall, B., 1987, Textural evidence for remobilization in metamorphic environments: Ore Geology Reviews, v. 2, p. 205-229.
- Grant, J. A., 1986, The isocon diagram; a simple solution to Gresens' equation for metasomatic alteration: Economic Geology, v. 81, p. 1976-1982.
- Grant, J. A., 2005, Isocon analysis: a brief review of the method and applications: Physics and Chemistry of the Earth, Parts A/B/C, v. 30, p. 997-1004.
- Gresens, R. L., 1967, Composition-volume relationships of metasomatism: Chemical geology, v. 2, p. 47-65.
- Ioannou, S., and Spooner, E., 2007, Fracture analysis of a volcanogenic massive sulfide-related hydrothermal cracking zone, Upper Bell River Complex, Matagami, Quebec: application of permeability tensor theory: Economic Geology, v. 102, p. 667-690.
- Ishikawa, Y., Sawaguchi, T., Iwaya, S., and Horiuchi, M., 1976, Delineation of prospecting targets for Kuroko deposits based on modes of volcanism of underlying dacite and alteration haloes: Mining Geology, v. 26, p. 105-117.
- Knuckey, M., Comba, C., and Riverin, G., 1982, Structure, metal zoning and alteration at the Millenbach deposit, Noranda, Quebec: Precambrian Sulphide

- Deposits, HS Robinson Memorial Volume, Geological Association of Canada Special paper, v. 25, p. 255-295.
- Lacroix, J., Daigneault, R., Chartrand, F., and Guha, J., 1993, Structural evolution of the Grevet Zn-Cu massive sulfide deposit, Lebel-sur-Quevillon area, Abitibi subprovince, Quebec: Economic Geology, v. 88, p. 1559-1577.
- Large, R. R., Gemmell, J. B., Paulick, H., and Huston, D. L., 2001, The alteration box plot: A simple approach to understanding the relationship between alteration mineralogy and lithogeochemistry associated with volcanic-hosted massive sulfide deposits: Economic Geology, v. 96, p. 957-971.
- Lavallière, G., Guha, J., and Daigneault, R., 1994, Cheminees de sulfures massifs atypiques du gisement d'Isle-Dieu, Matagami, Quebec; implications pour l'exploration: Exploration and Mining Geology, v. 3, p. 109-129.
- Liaghat, S., and MacLean, W. H., 1992, The Key Tuffite, Matagami mining district; origin of the tuff components and mass changes: Exploration and Mining Geology, v. 1, p. 197-207.
- Lydon, J. W., 1984, Ore Deposit Models-8. Volcanogenic Massive Sulphide Deposits Part I: A Descriptive Model: Geoscience Canada, v. 11.
- MacGeehan, P. J., and MacLean, W. H., 1980, Tholeiitic basalt-rhyolite magmatism and massive sulphide deposits at Matagami, Quebec: Nature, v. 283, p. 153-157.
- MacLean, W., 1984, Geology and ore deposits of the Matagami District: Chibougamau Stratigraphy and Mineralization. Guha, J. and Chown, E.H., (Eds.), CIM Special, v. 34, p. 483-495.
- MacLean, W., 1990, Mass change calculations in altered rock series: Mineralium Deposita, v. 25, p. 44-49.
- MacLean, W., and Barrett, T., 1993, Lithogeochemical techniques using immobile elements: Journal of geochemical exploration, v. 48, p. 109-133.
- MacLean, W., and Kranidiotis, P., 1987, Immobile elements as monitors of mass transfer in hydrothermal alteration; Phelps Dodge massive sulfide deposit, Matagami, Quebec: Economic Geology, v. 82, p. 951-962.
- Maier, W., Barnes, S.-J., and Pellet, T., 1996, The economic significance of the Bell River Complex, Abitibi subprovince, Quebec: Canadian Journal of Earth Sciences, v. 33, p. 967-980.
- Marshall, B., and Gilligan, L., 1993, Remobilization, syn-tectonic processes and massive sulphide deposits: Ore Geology Reviews, v. 8, p. 39-64.

- Marshall, B., and Gilligan, L. B., 1987, An introduction to remobilization: information from ore-body geometry and experimental considerations: *Ore Geology Reviews*, v. 2, p. 87-131.
- Marshall, B., and Gilligan, L. B., 1989, Durchbewegung structure, piercement cusps, and piercement veins in massive sulfide deposits; formation and interpretation: *Economic Geology*, v. 84, p. 2311-2319.
- McClay, K., and Ellis, P., 1983, Deformation and recrystallization of pyrite: *Mineralogical Magazine*, v. 47, p. 527-538.
- McDonald, J. A., 1970, Some effects of deformation on sulfide-rich layers in lead-zinc ore bodies, Mount Isa, Queensland: *Economic Geology*, v. 65, p. 273-298.
- McPhie, J., Doyle, M., Allen, R., and Allen, R. L., 1993, Volcanic textures: a guide to the interpretation of textures in volcanic rocks: Hobart, Australia, Centre for Ore Deposit and Exploration Studies, University of Tasmania, 198 p.
- McQueen, K., 1987, Deformation and remobilization in some Western Australian nickel ores: *Ore Geology Reviews*, v. 2, p. 269-286.
- Mercier-Langevin, P., McNicoll, V., Allen, R. L., Blight, J. H., and Dubé, B., 2013, The Boliden gold-rich volcanogenic massive sulfide deposit, Skellefte district, Sweden: new U-Pb age constraints and implications at deposit and district scale: *Mineralium Deposita*, v. 48, p. 485-504.
- Mortensen, J. K., 1993, U-Pb geochronology of the eastern Abitibi Subprovince. Part 1: Chibougamau-Matagami-Joutel region: *Canadian Journal of Earth Sciences*, v. 30, p. 11-28.
- Piché, M., Guha, J., and Daigneault, R., 1993, Stratigraphic and structural aspects of the volcanic rocks of the Matagami mining camp, Quebec; implications for the Norita ore deposit: *Economic Geology*, v. 88, p. 1542-1558.
- Pilote, P., Debreil, J.-A., Williamson, K., Rabeau, O., and Lacoste, P., 2011, Revision géologique de la région de Matagami, Québec Exploration, poster 276, Québec, Canada.
- Riverin, G., and Hodgson, C., 1980, Wall-rock alteration at the Millenbach Cu-Zn mine, Noranda, Quebec: *Economic Geology*, v. 75, p. 424-444.
- Roberts, R. G., 1975, The geological setting of the Mattagami Lake Mine, Quebec; a volcanogenic massive sulfide deposit: *Economic Geology*, v. 70, p. 115-129.
- Ross, P.-S., McNicoll, V. J., Debreil, J.-A., and Carr, P., 2014, Precise U-Pb Geochronology of the Matagami Mining Camp, Abitibi Greenstone Belt,

- Quebec: Stratigraphic Constraints and Implications for Volcanogenic Massive Sulfide Exploration: Economic Geology, v. 109, p. 89-101.
- Sharpe, J.I., 1968, Geology and sulfide deposits of the Matagami area, Abitibi-East County: Geological Report 137, Ressources Naturelles Quebec, 122 p.
- Shriver, N., and MacLean, W., 1993, Mass, volume and chemical changes in the alteration zone at the Norbec mine, Noranda, Quebec: Mineralium deposita, v. 28, p. 157-166.
- Vokes, F., and Craig, J., 1993, Post-recrystallisation mobilisation phenomena in metamorphosed stratabound sulphide ores: Mineralogical Magazine, London, v. 57, p. 19-19.
- Vokes, F. M., 1973, "Ball texture" in sulphide ores: GFF, v. 95, p. 403-406.

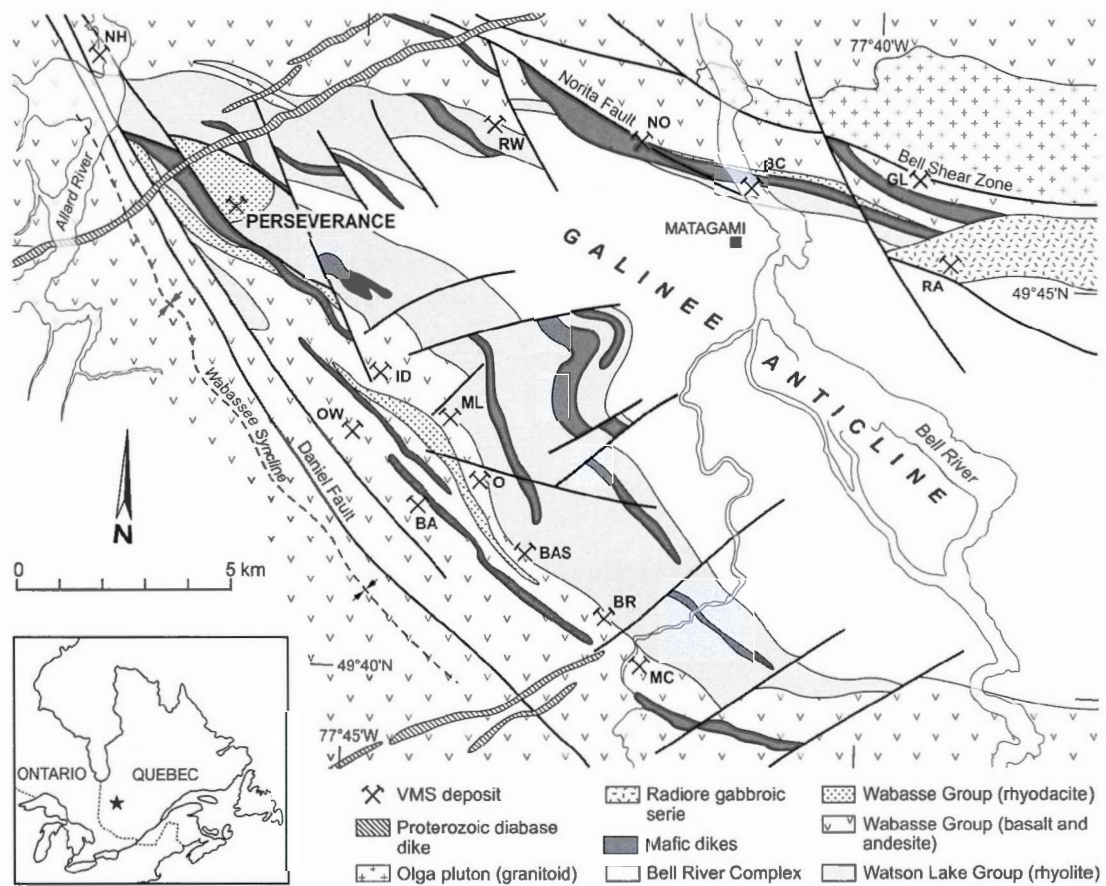


Fig. 1.1. Geologic map of the Matagami district (modified from Pilote et al., 2011). North flank deposits: BC = Bell Channel, GL = Garon Lake, NH = New Hosco, NO = Norita, RA = Radiore, RW = Radiore West. South flank deposits: BA = Bell Allard, BAS = Bell Allard South, BR = Bracemac, ID = Isle Dieu, MC = McLeod, ML = Matagami Lake, O = Orchan, OW = Orchan West.

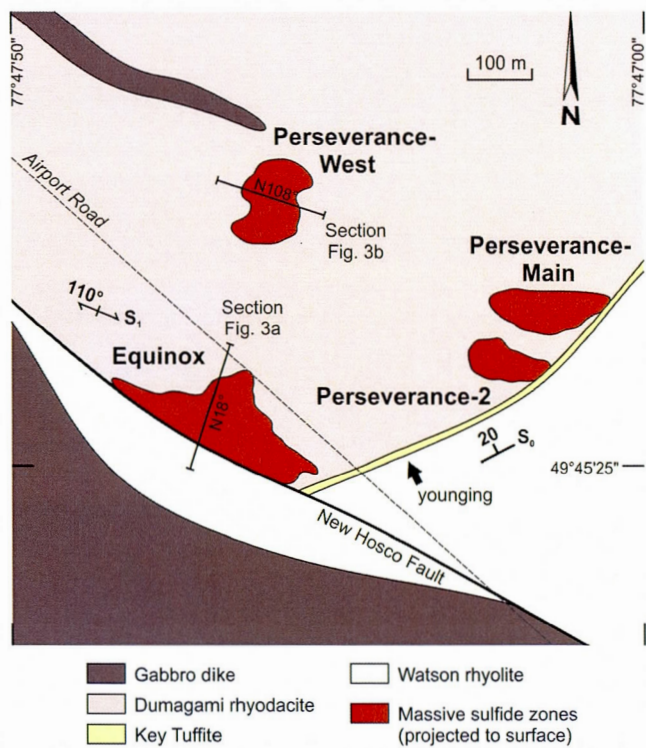


Fig. 1.2. Simplified geologic surface map of the Perseverance deposit vicinity showing the ore distribution (projected from level 130) and main lithologies. Modified from unpublished Glencore Canada Corporation map.

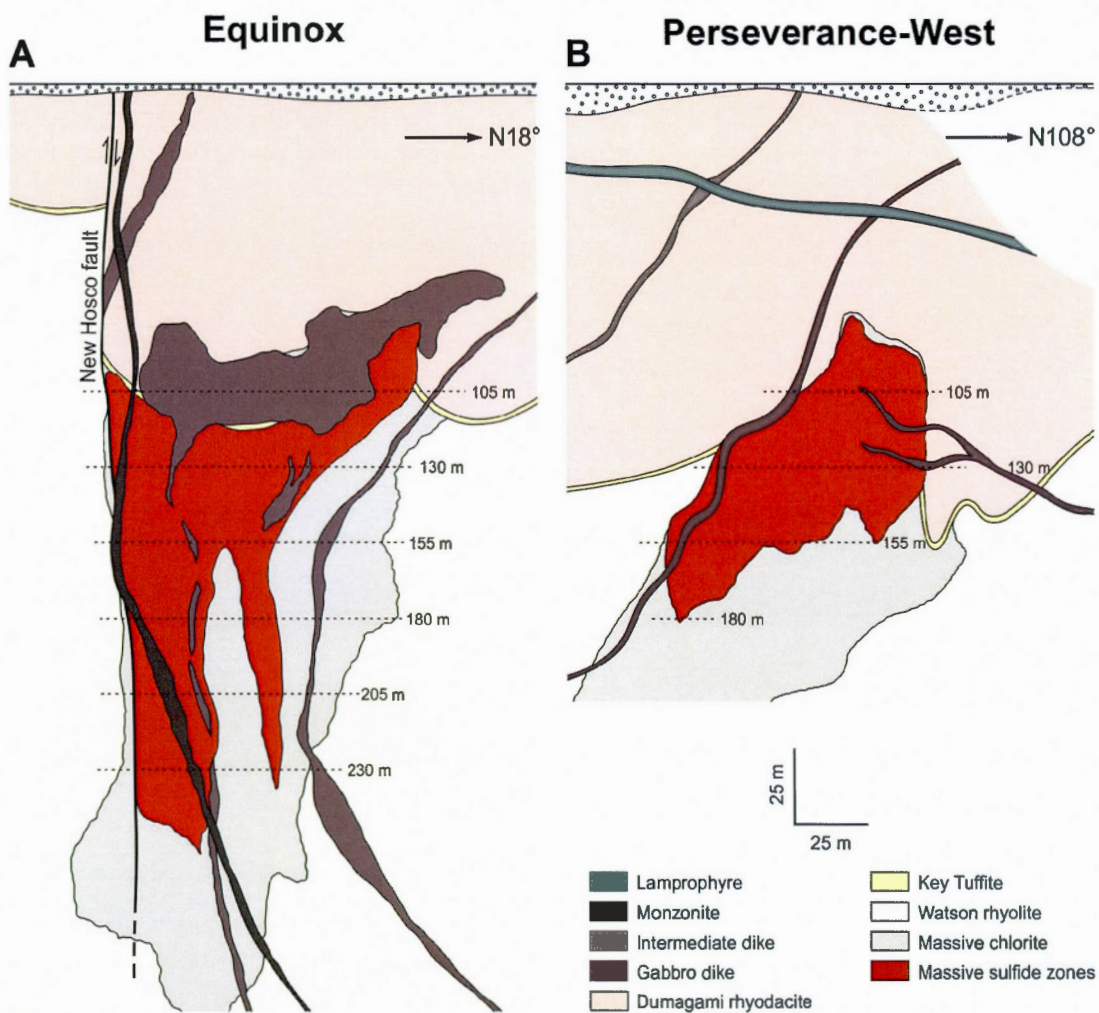


Fig. 1.3. Simplified geologic sections through the Equinox (A) and Perseverance-West (B) orebodies showing the inferred schematic distribution of the principal units that host the deposit, the ore lenses (production levels are indicated) and associated chlorite alteration zones. Modified from unpublished Glencore Canada Corporation sections.

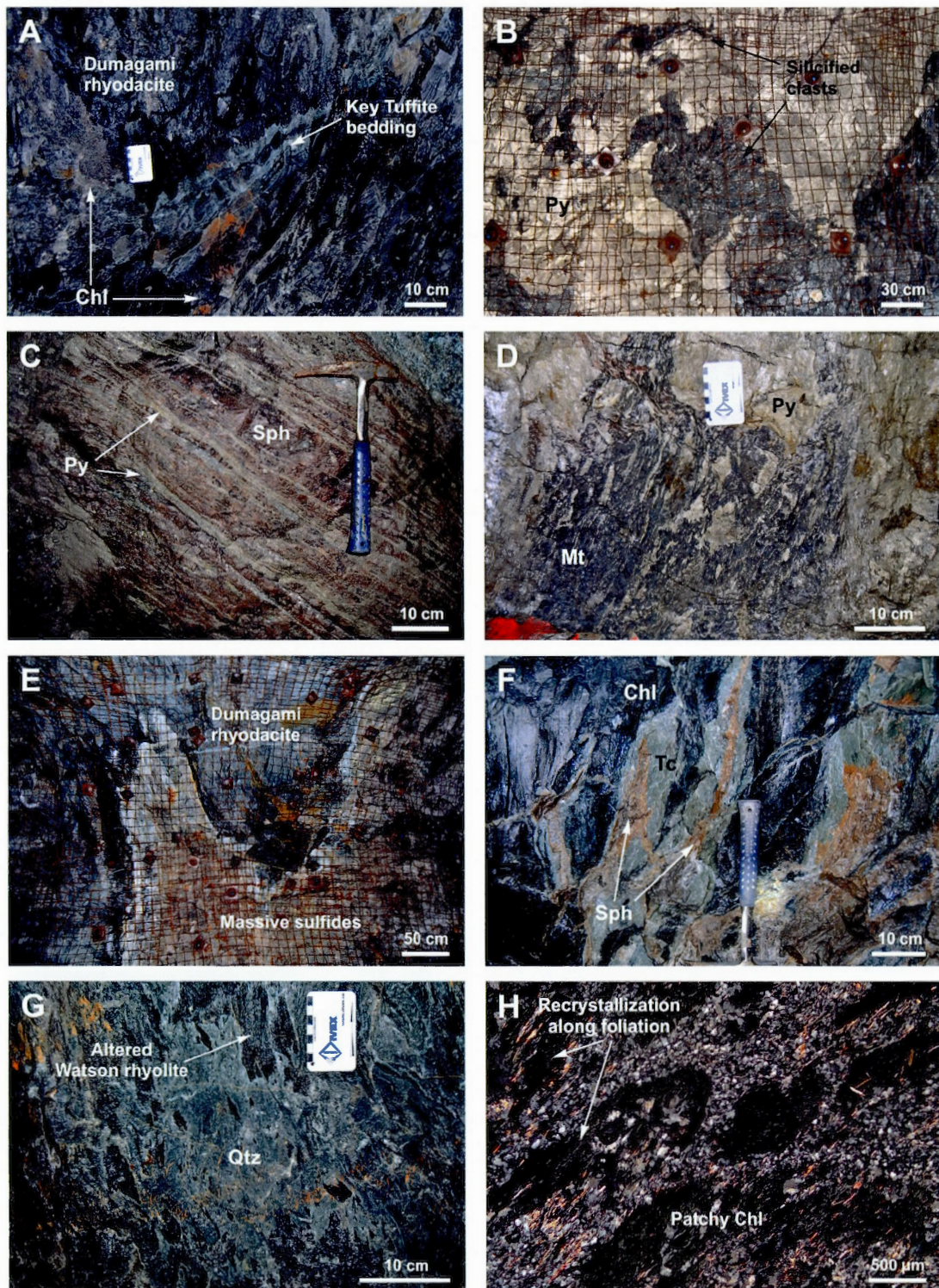


Fig. 1.4. A. Section view of the Key Tuffite upper contact with the hanging wall Dumagami rhyodacite, obliterated by strong pervasive chlorite alteration, stope 70-

P2-Accès. B. Altered host rock fragments enclosed within pyritic massive sulfide ore, stope 105-EQ-23. C. Plan view of typical sphalerite-rich banded ore, stope 105-EQ-20. D. Magnetite-rich facies in contact with massive pyritic ore, stope 105-EQ-18. E. Upper portion of the massive sulfides in direct contact with the hanging wall Dumagami rhyodacite, stope 105-PW-16. F. Strong talc-chlorite alteration in close spatial relationship with sphalerite-rich veins, stope 105-PW-18. G. Pervasive quartz alteration in foliated Watson rhyolite, stope 130-EQ-access. H. Patchy hydrothermal chlorite showing recrystallization and realignment parallel to foliation, photomicrograph in transmitted light, drill hole PER-00-20. Abbreviations: Chl = chlorite, Mt = magnetite, Py = pyrite, Qtz = quartz, Sph = sphalerite, Tc = talc; EQ = Equinox, P2 = Perseverance-2, PW = Perseverance-West.

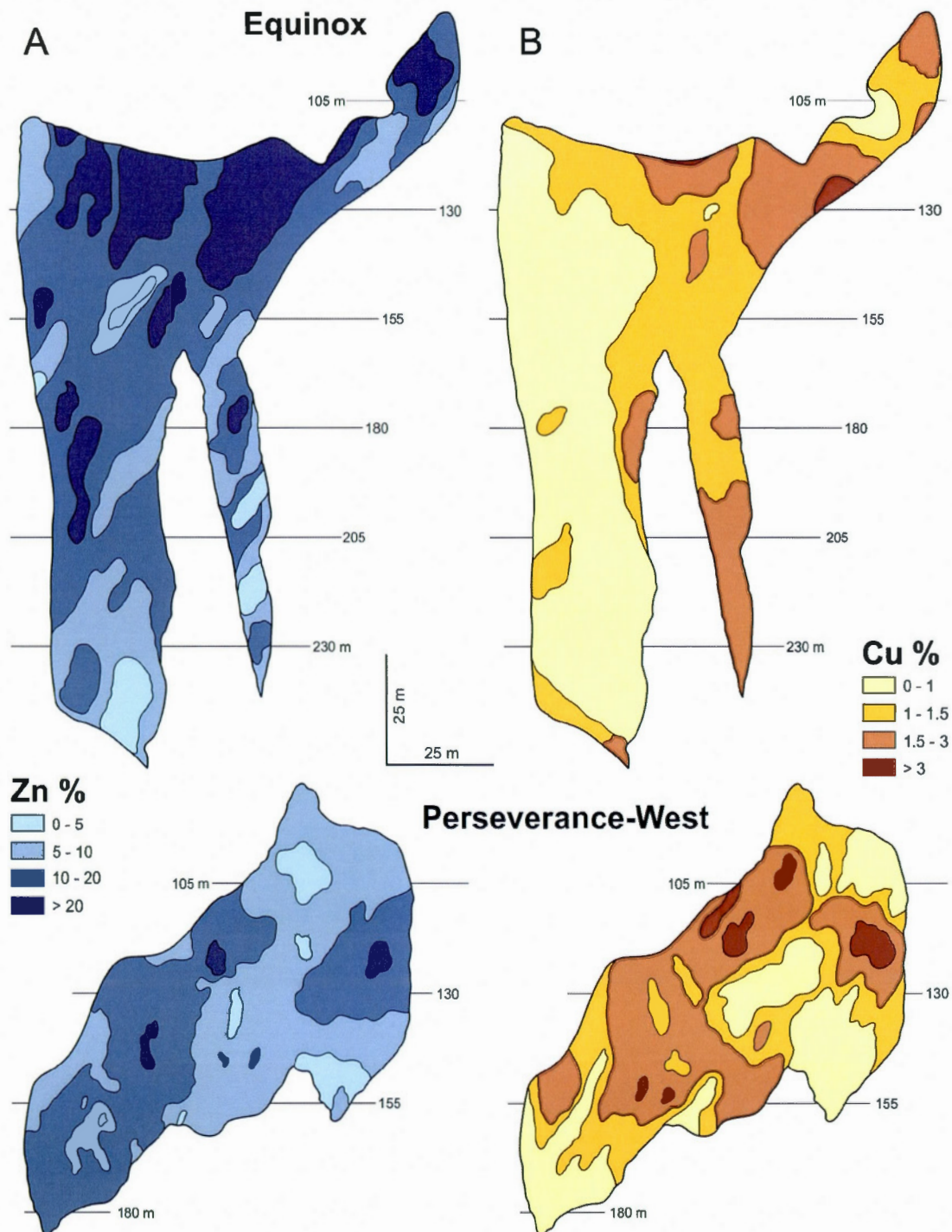


Fig. 1.5. Vertical sections showing the zinc and copper distributions of Equinox (looking west) and Perseverance-West (looking north) orebodies. From unpublished Glencore Canada Corporation block model resource estimate.

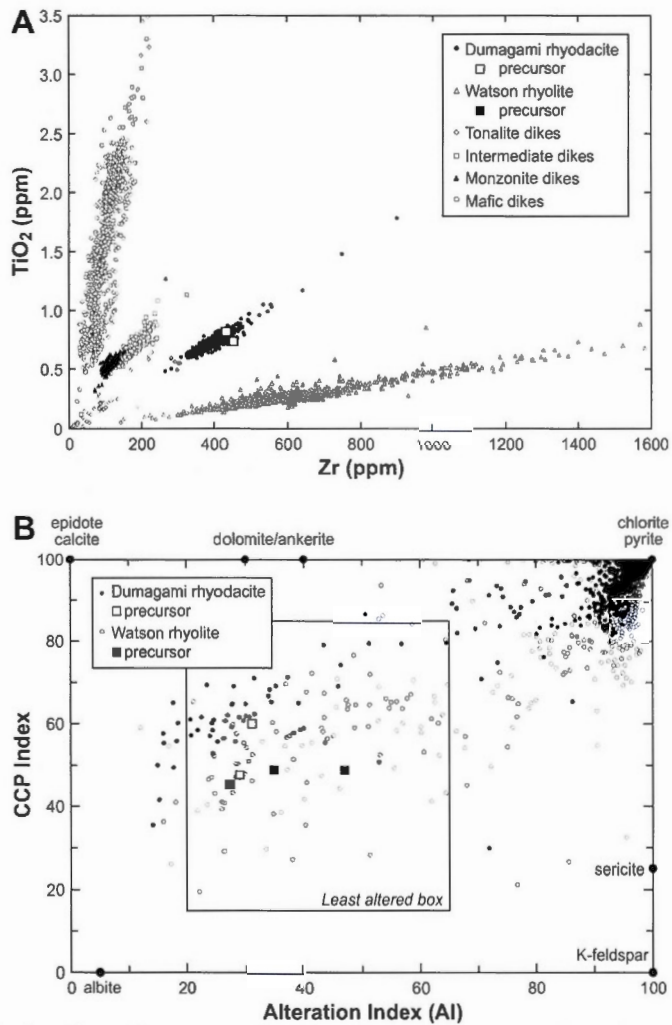


Fig. 1.6. Discrimination diagrams for the Perseverance volcanic rocks. A. TiO₂-Zr plot showing the different trends relating to varying Ti/Zr ratios for major lithologies and associated alteration lines linking samples of similar precursor composition. B. Alteration index (AI)-chlorite-carbonate-pyrite index (CCPI) box plot showing hydrothermal alteration trends in the immediate vicinity of Perseverance (from Large et al., 2001). AI = 100(MgO + K₂O)/ (MgO + K₂O + Na₂O + CaO), CCPI = 100(FeO + MgO)/ (FeO + MgO + Na₂O + K₂O)

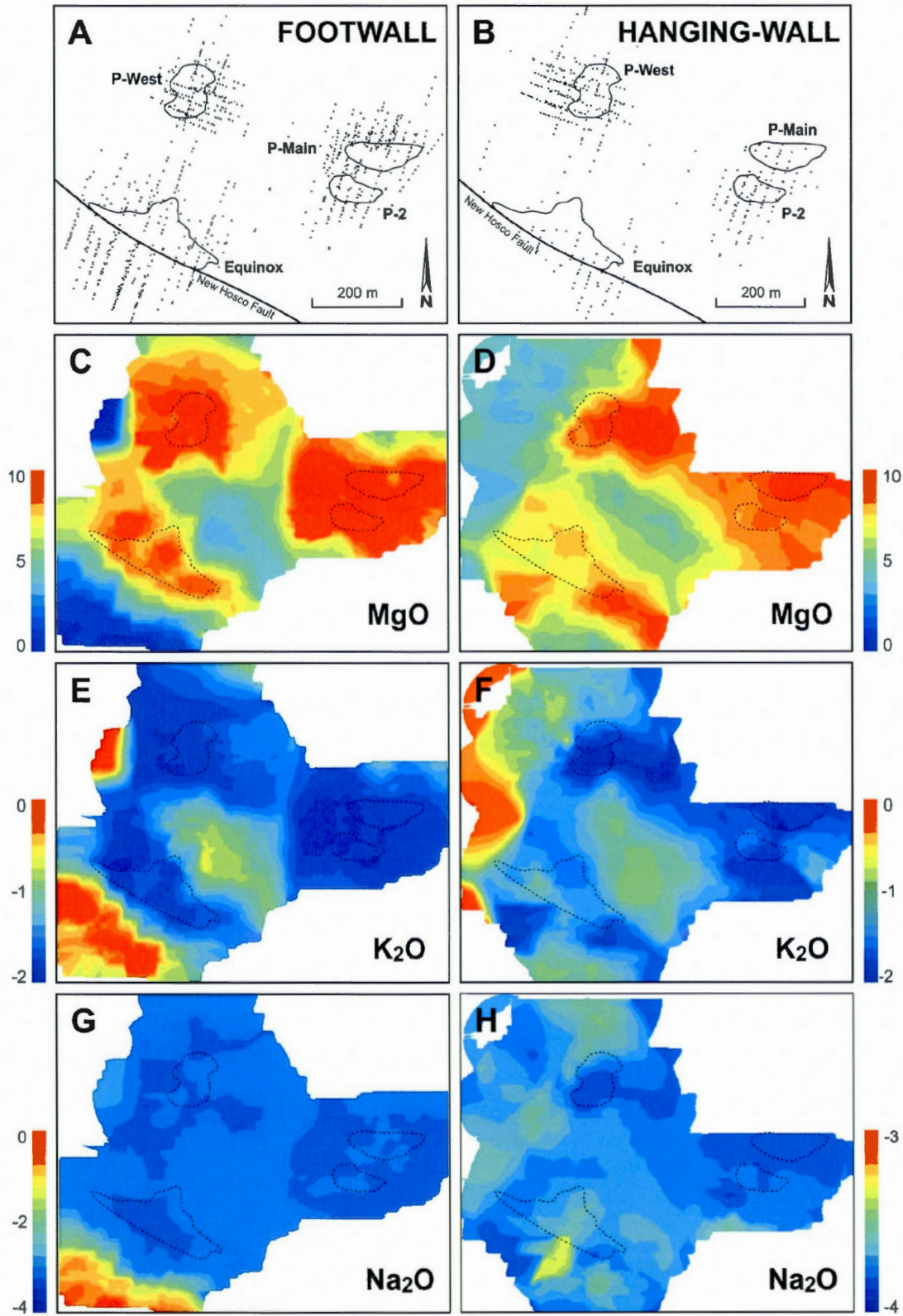


Fig. 1.7. Plan view showing the relationship between mass balance calculations (in wt%) for representative mobile elements and the location of the orebodies at Perseverance. A. Data points of the footwall Watson rhyolite. B. Data points of the hanging wall Dumagami rhyodacite. C. and D. Mass changes in MgO. E. and F. Mass changes in K₂O. G. and H. Mass changes in Na₂O.

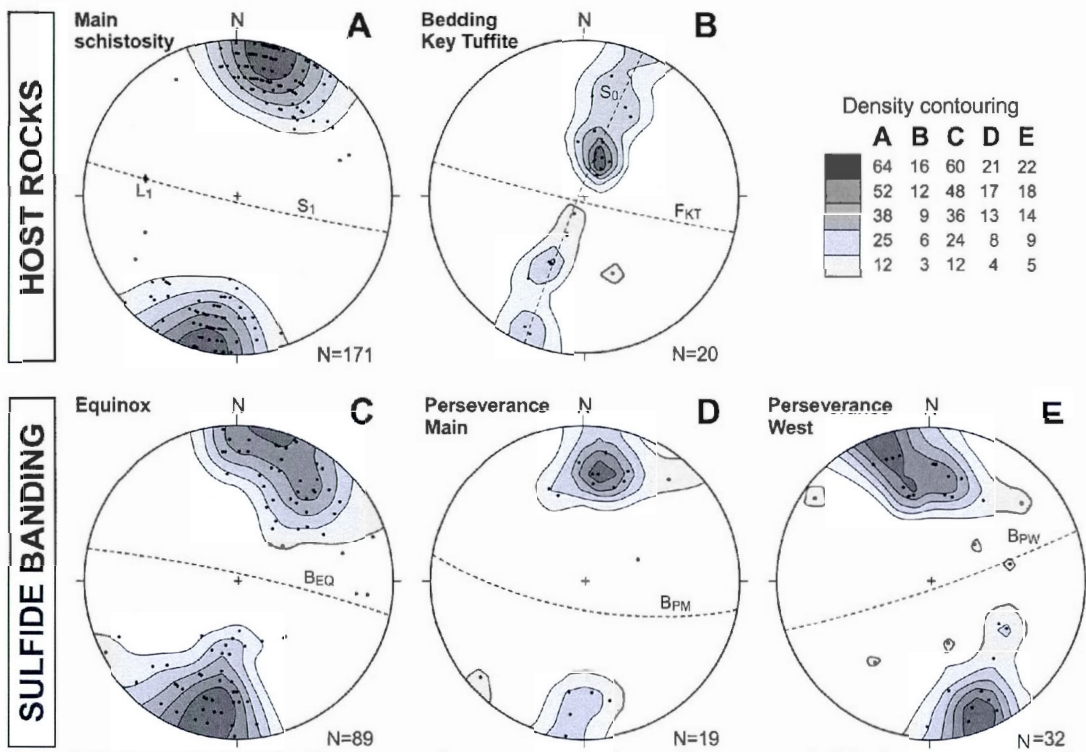


Fig. 1.8. Lower hemisphere equal-area projection of measured fabrics in host rocks versus ore envelopes. A. Main schistosity (S_1) measured in moderately to strongly altered volcanic host rocks. B. Average axial plane (F_{KT}) of folds developed in the Key Tuffite unit. C., D. and E. Average attitude of the ribbon texture in the Equinox (B_{EQ}), Perseverance-Main (B_{PM}) and Perseverance-West (B_{PW}) orebodies.

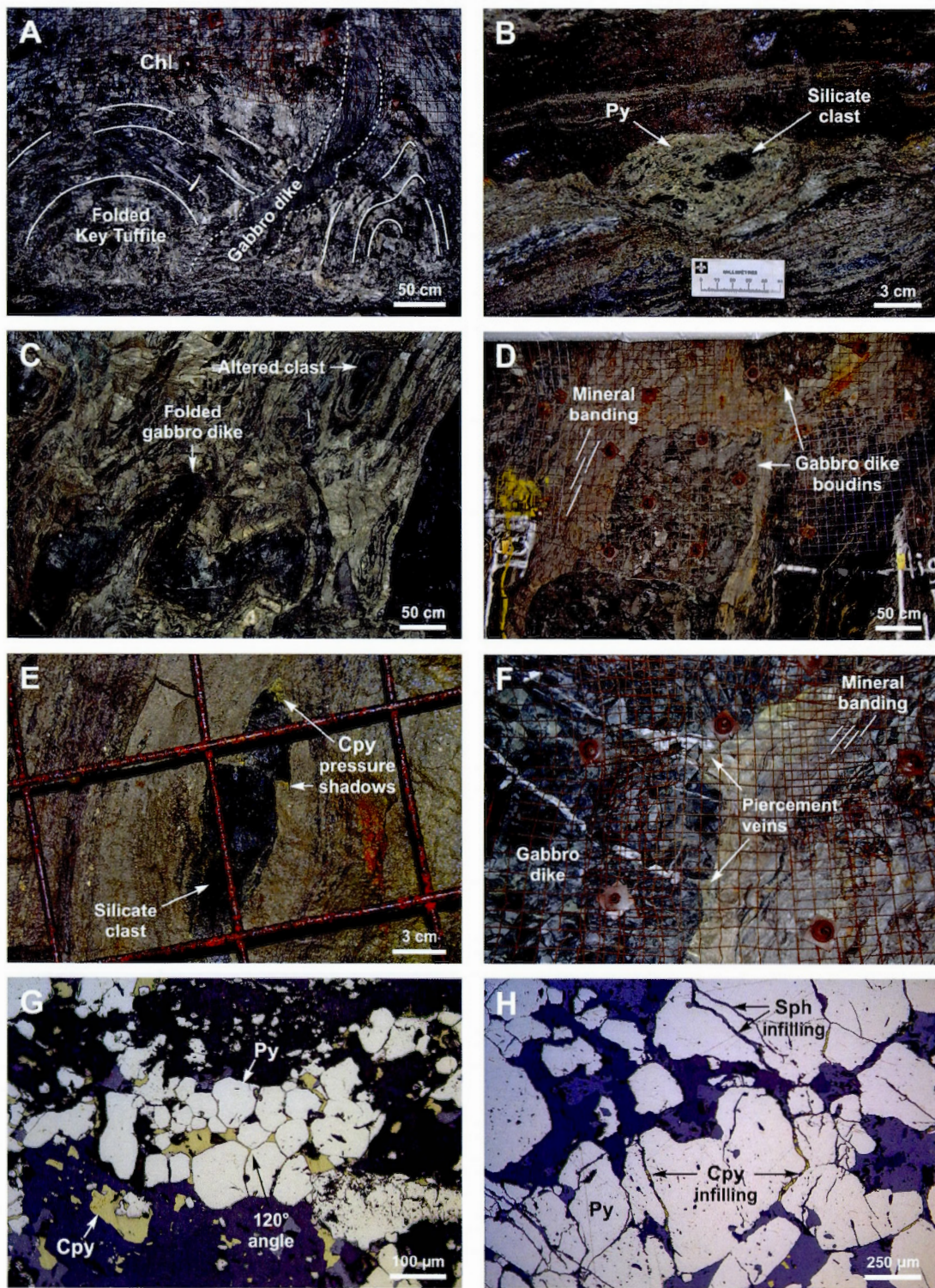


Fig. 1.9. A. Open to isoclinal folds developed by the Key Tuffite unit at the contact with the Dumagami rhyodacite; intense chlorite alteration pervasive throughout the

units, stope 105-P2-01. B. Plan view of durchbewegung structure with pyrite and silicate fragments showing internal rotations in a matrix of banded pyrite-sphalerite ore, stope 105-EQ-18. C. Section view of gabbro dike affected by isoclinal folding in massive pyrite-sphalerite ore, stope 130-EQ-25. D. Gabbro dike affected by metric boudinage parallel to the direction of the ribbon-textured ore, stope 130-EQ-18. E. Chalcopyrite pressure shadows developed at the extremities of a boudinaged silicate clast in the banded ore facies. F. Piercement veins developed at the interface between a gabbro dike and massive sulfides, stope 105-EQ-18. G. Equidimensional pyrite grains displaying triple junctions with 120° dihedral angles, photomicrograph in reflected light, 105-EQ-18. H. Highly fractured pyrite grains infilled by chalcopyrite and sphalerite, photomicrograph in reflected light, 105-EQ-18. Abbreviations: Chl = chlorite, Cpy = chalcopyrite, Py = pyrite, Sph = sphalerite; EQ = Equinox, P2 = Perseverance-2, PW = Perseverance-West.

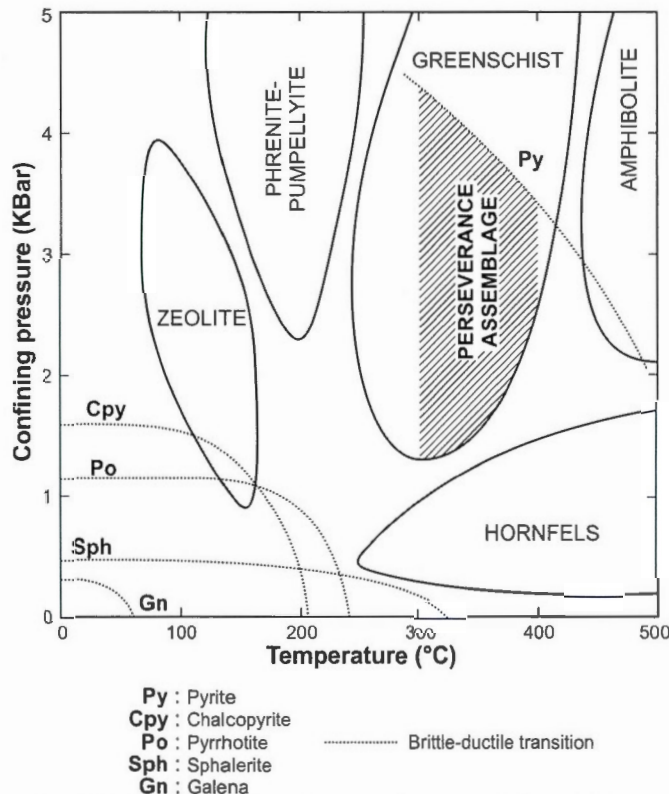


Fig. 1.10. Mechanical behavior of common base-metal sulfides with their brittle-ductile transitions at 5% ductile strain before faulting and indicative position of the Perseverance assemblage between 300°C and 400°C in the greenschist facies (modified from Marshall and Gilligan, 1987).

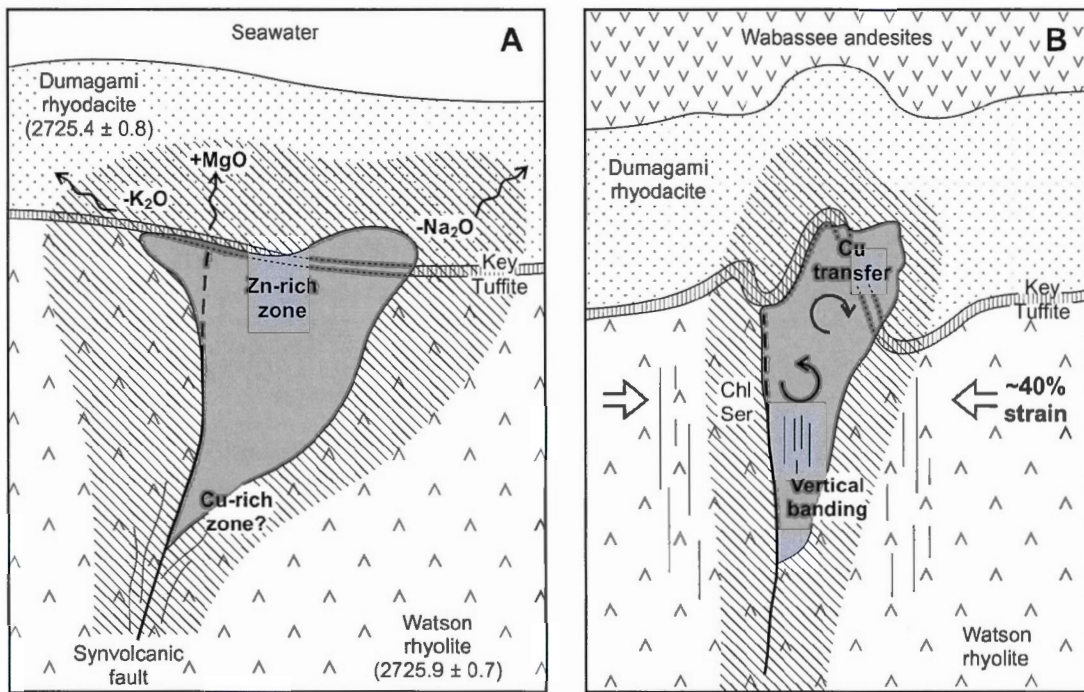


Fig. 1.11. Schematic north-south section, showing the possible predeformation architecture of the mineralized hydrothermal system in the Perseverance deposit and the subsequent structural and compositionnal modifications induced during regional greenschist facies metamorphism.

TABLE 1.1. Geochemical Compositions of the Volcanic Units and their Respective Precursors

Facies Sample	Altered footwall		Precursors footwall			Altered hanging wall		Precursors hanging wall	
	n=1066		34971	34969	67051M	n=645		862161	
	Avg.	Std. dev.				Avg.	Std. dev.		
Major oxides¹ (%)									
SiO ₂	67.40	13.06	75.79	74.61	75.2	69.11	4.94	74.4	72.23
TiO ₂	0.27	0.10	0.24	0.28	0.26	0.73	0.08	0.74	0.82
Al ₂ O ₃	10.33	3.23	10.74	11	10.6	10.60	1.2	11.58	10.85
Fe ₂ O ₃	6.80	3.94	4.05	4.32	4.32	6.36	2.17	3.62	5.98
MnO	0.04	0.04	0.08	0.08	0.06	0.04	0.03	0.07	0.06
MgO	8.46	6.18	0.6	1.16	0.78	6.80	3.08	0.98	1.41
CaO	0.36	0.73	1.62	1.32	1.99	0.45	0.73	1.69	1.28
Na ₂ O	0.42	0.96	3.68	2.8	2.97	0.45	1.01	3.63	3.67
K ₂ O	0.59	0.81	1.39	2.5	1.88	0.51	0.47	1.18	0.83
P ₂ O ₅	0.05	0.05	0.03	0.03	0.02	0.14	0.26	0.14	0.16
LOI	4.49	2.29	0.83	0.84	1.2	4.10	1.62	1.89	1.92
Total	99.23	0.55	99.12	99.03	99.5	99.31	0.47	99.98	99.3
Ratios and alteration indices									
Al ₂ O ₃ /TiO ₂	38.58	3.67	44.75	39.29	40.46	14.61	0.74	15.65	13.23
TiO ₂ /Zr	4.44	0.49	3.95	4.11	4.25	18.28	0.68	16.41	18.94
Zr/Y	4.28	1.49	3.5	3.7	3.7	3.55	0.49	3.5	2.5
Al ²	90.74	17.39	27.30	47.04	34.91	88.83	18.82	28.88	31.15
CCPI ²	90.37	15.11	45.57	48.78	49.04	91.74	10.98	46.84	60.15

¹ Major and trace elements performed by X-Ray fluorescence
² Alteration Index (AI) from Ishikawa et al. (1976)

³ Chlorite-carbonate-pyrite index (Large et al., 2001)

CONCLUSION GÉNÉRALE

Le gisement de Persévérence est composé de quatre lentilles de sulfures massifs riches en zinc, globalement perpendiculaires à une séquence volcanique de faible pendage (20° NW). L'étude détaillée du gisement apporte une meilleure compréhension sur les mécanismes de mise en place des amas sulfurés au cours du volcanisme à Matagami et suggère que d'importantes modifications structurales ont affecté l'architecture originale dans le flanc sud du district.

Le gisement est interprété comme ayant été formé par remplacement sous fond marin au travers des éléments suivants: 1) relation discordante entre les lentilles et la stratigraphie, 2) présence de reliques des roches encaissantes au sein des enveloppes minéralisées, 3) intense altération pervasive dans le toit du gisement, et 4) mise en place rapide de la séquence volcanique. La genèse des quatre lentilles est probablement reliée à des contrastes de perméabilité au sein de l'assemblage volcanique et contrôlée par des porosités primaires et structurales développées dans les unités. Cet assemblage syn-volcanique a été repris par une intense déformation au cours du métamorphisme régional au faciès des schistes verts. La déformation est contrôlée par des contrastes de compétence, liés à des différences de ductilité au sein de l'assemblage polymétallique et vis-à-vis des roches encaissantes silicatées. Outre des modifications globales de géométrie, de nombreuses textures et structures reflètent la déformation, incluant un rubanement vertical des sulfures, un boudinage prononcé des dykes mafiques, de nombreux plis, ainsi que des structures de percement et de type "durchbewegung". Une remobilisation structurale de la chalcopyrite est suggérée et implique que la zonalité originelle du cuivre a été modifiée au cours de l'épisode de métamorphisme.

Plusieurs aspects documentés à Persévérence fournissent de potentiels guides d'exploration pour la recherche des amas sulfurés au sein du district et dans des environnements similaires. Une altération pervasive au toit des lentilles constitue un élément important de la mise en place du gisement. En conséquence, la présence

d'enrichissements en magnésium combinée avec le lessivage des éléments alcalins doit être examinée avec attention au toit des cibles et préférentiellement dans les zones de pendage faible à modéré. De plus, les zones d'altération en chlorite ont favorablement accommodé les contraintes de par leur ductilité. En conséquence, les halos d'altération hydrothermale sont spatialement corrélés avec les zones de déformation, malgré l'absence de lien génétique. La reconnaissance de déformations ductiles au sein d'horizons fertiles - tels que des plis dans la Tuffite Clé - en relation avec les zones d'altération, présente un potentiel certain pour l'exploration.

APPENDICE A

MODÉLISATION 3D DU GISEMENT DE PERSÉVÉRANCE

Introduction

Une modélisation 3D du gisement de Persévérence a été réalisée afin de visualiser les relations spatiales et structurales des zones minéralisées au sein de l'encaissant volcanique. Cette modélisation permet de les contraindre en intégrant la distribution des lithologies encaissantes et des zones minéralisées, la géochimie des altérations, ainsi que les zonalités en métaux des lentilles. Le travail a été effectué à l'aide du logiciel Leapfrog Mining 3D (ARANZ Geo), et est permis en particulier par la forte densité des données de mise en valeur du gisement (forages d'exploration et de définition) de Glencore Canada Corporation.

Méthode

Le gisement de Persévérence a fait l'objet de 270 forages de définition (63532 m), ainsi que de 344 forages souterrains en "éventail" pour sa mise en production (Arnold, 2006). Ces campagnes ont permis de constituer une base de données de 24 235 analyses métallurgiques (Zn, Cu, Pb, ± Au), ainsi que 2807 analyses de roche totale (éléments majeurs, ± traces). Les analyses en éléments majeurs ont été utilisées dans la présente étude pour générer 1709 calculs de bilan de masse au sein de la rhyolite de Watson et de la rhyodacite de Dumagami. Dans le modèle présenté ci-dessous, les données lithologiques (log) de forages ont été utilisées pour la représentation des unités hôtes, de la minéralisation, des zones de magnétite massive ainsi que des zones de forte chloritisation ou "pipe d'altération" via une représentation qualitative de leur volume (i.e., "litho boundaries"). Les zonalités en zinc et en cuivre au sein des zones minéralisées ainsi que la représentation des bilans de masse ont fait l'objet d'interpolations numériques en fonction de leurs valeurs (i.e., "assay numeric datas").

Résultats

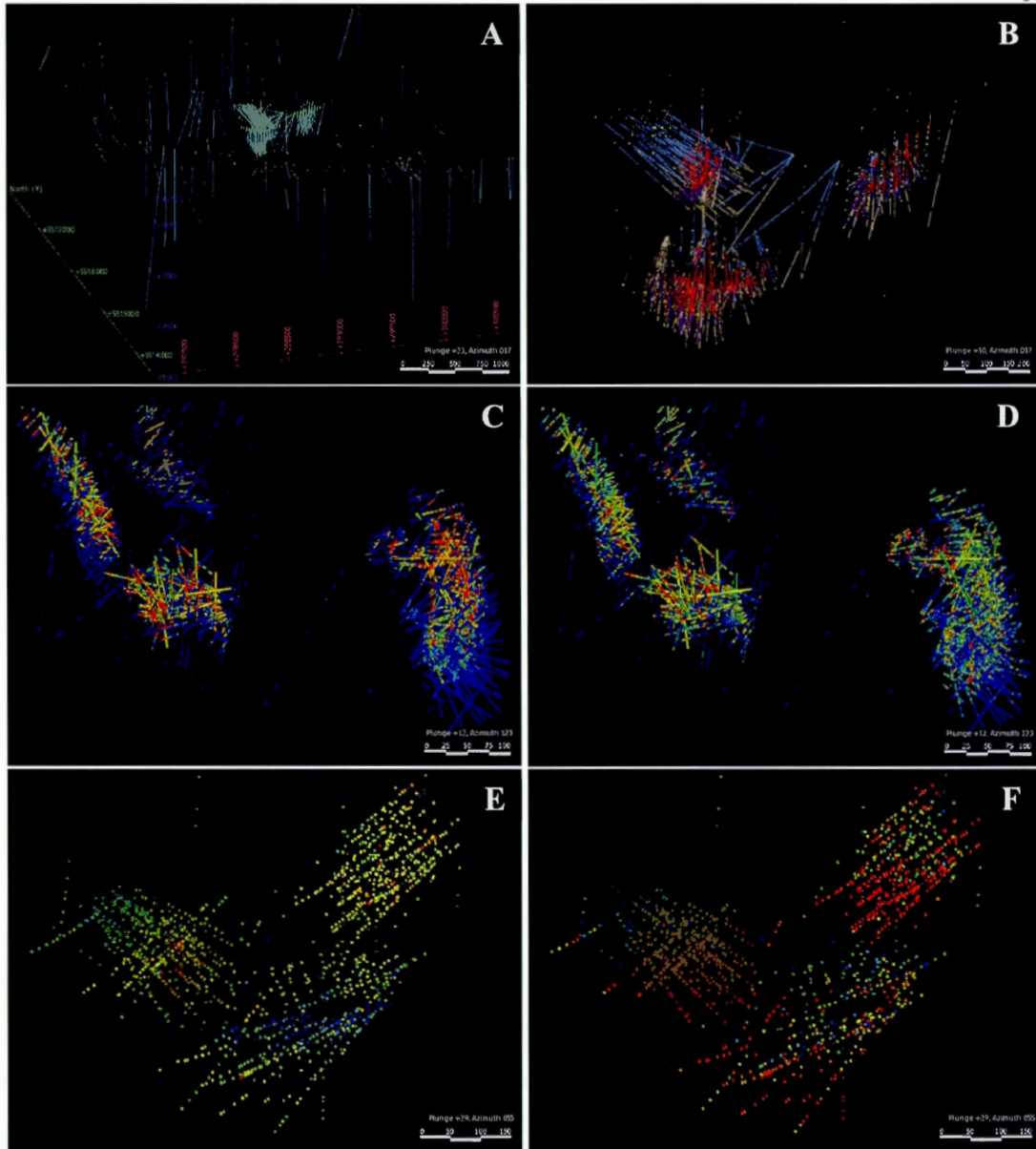


Figure A.1. Répartition des données importées avant modélisation. (A) Distribution de l'ensemble des forages du secteur de Persévérence avec les forages historiques en périphérie de la zone de définition du gisement, *vue NNE*. (B) Zone de définition du gisement avec lithologies illustrant les trois zones principales, *vue NNE*. (C) Distribution des analyses en zinc, *vue SE*. (D) Distribution des analyses en cuivre, *vue SE*. (E) Distribution des valeurs de bilan de masse en MgO, *vue NE*. (F) Distribution des valeurs de bilan de masse en K₂O, *vue NE*.

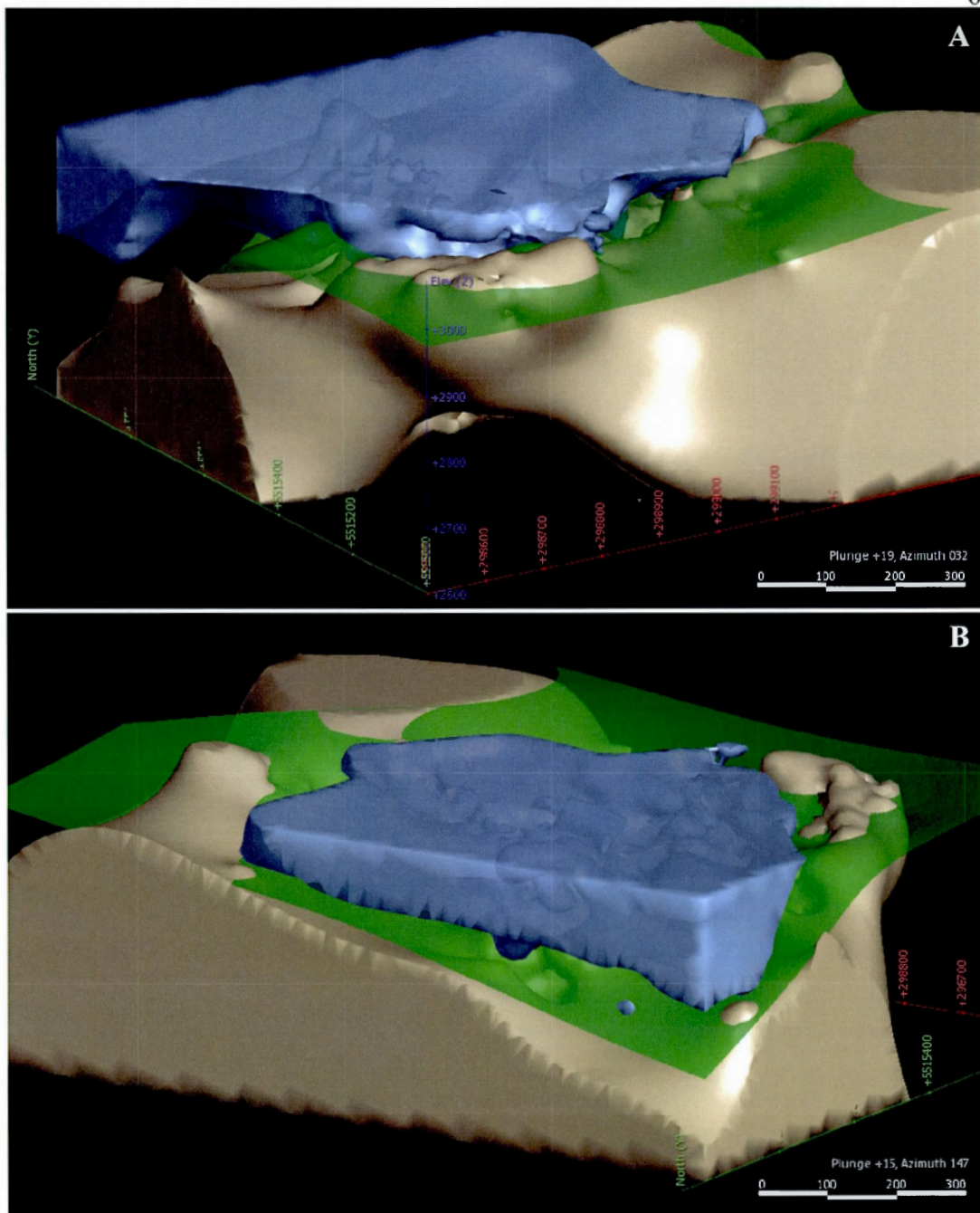


Figure A.2. Modèle 3D de la séquence volcanique hôte du gisement de Persévérence, incluant la rhyolite de Watson (beige), la Tuffite Clé (vert) et la rhyodacite de Dumagami (bleu). Dimensions du bloc: X=1200 m, Y=1000 m, Z=400 m. (A) Vue vers le NE. (B) Vue vers le SE.

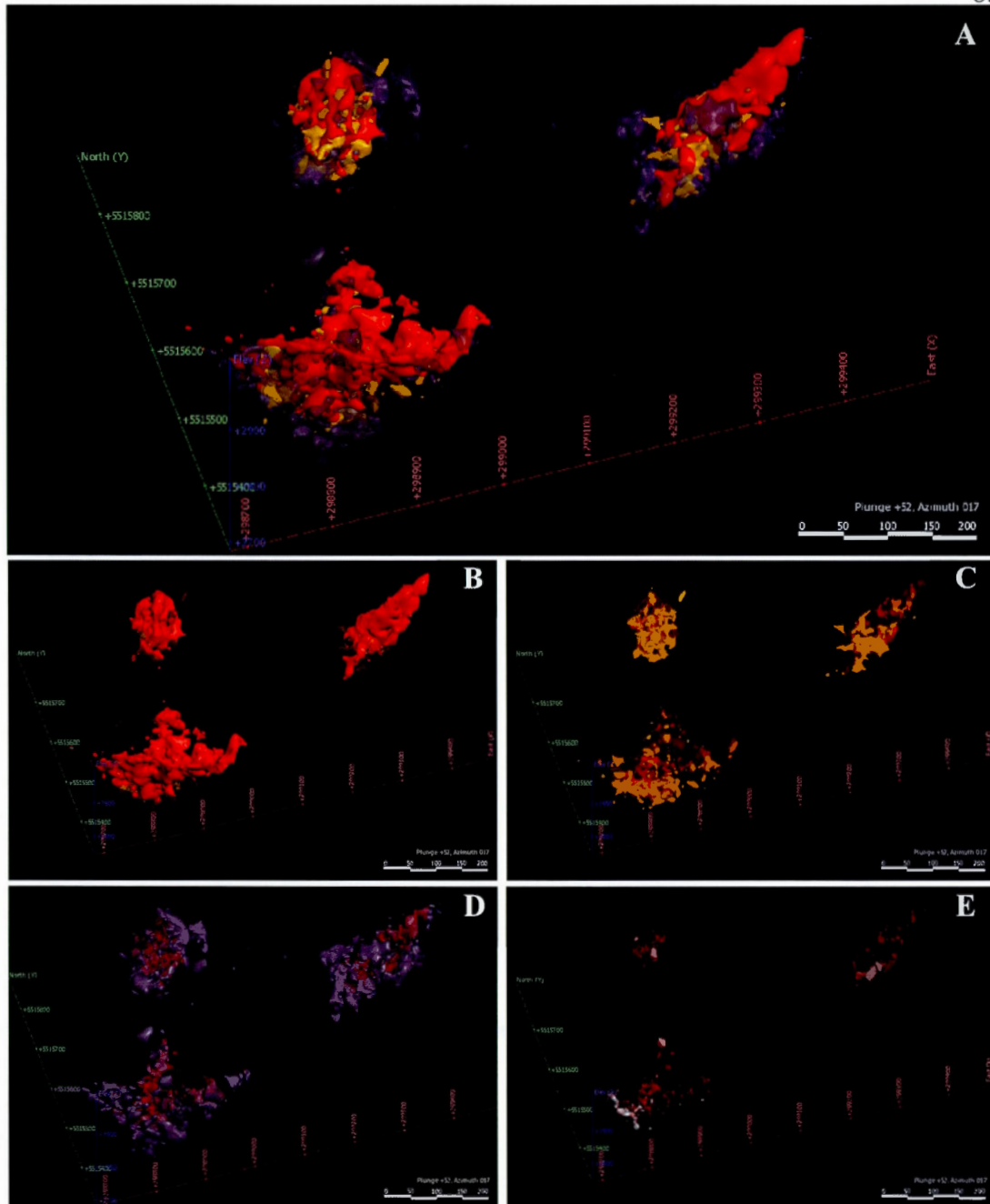


Figure A.3. Modèle 3D des zones minéralisées du gisement de Persévérance, incluant les sulfures massifs (rouge), les sulfures semi-massifs (orange), les zones de forte chloritisation ou "pipe d'altération" (violet) et la magnétite massive (blanc) (A) Relation entre des différents types, caractérisant les trois zones minéralisées. Distribution de: (B) sulfures massifs, (C) sulfures semi-massifs, (D) forte chloritisation et (E) magnétite massive. Toutes les vues sont vers le NNE.

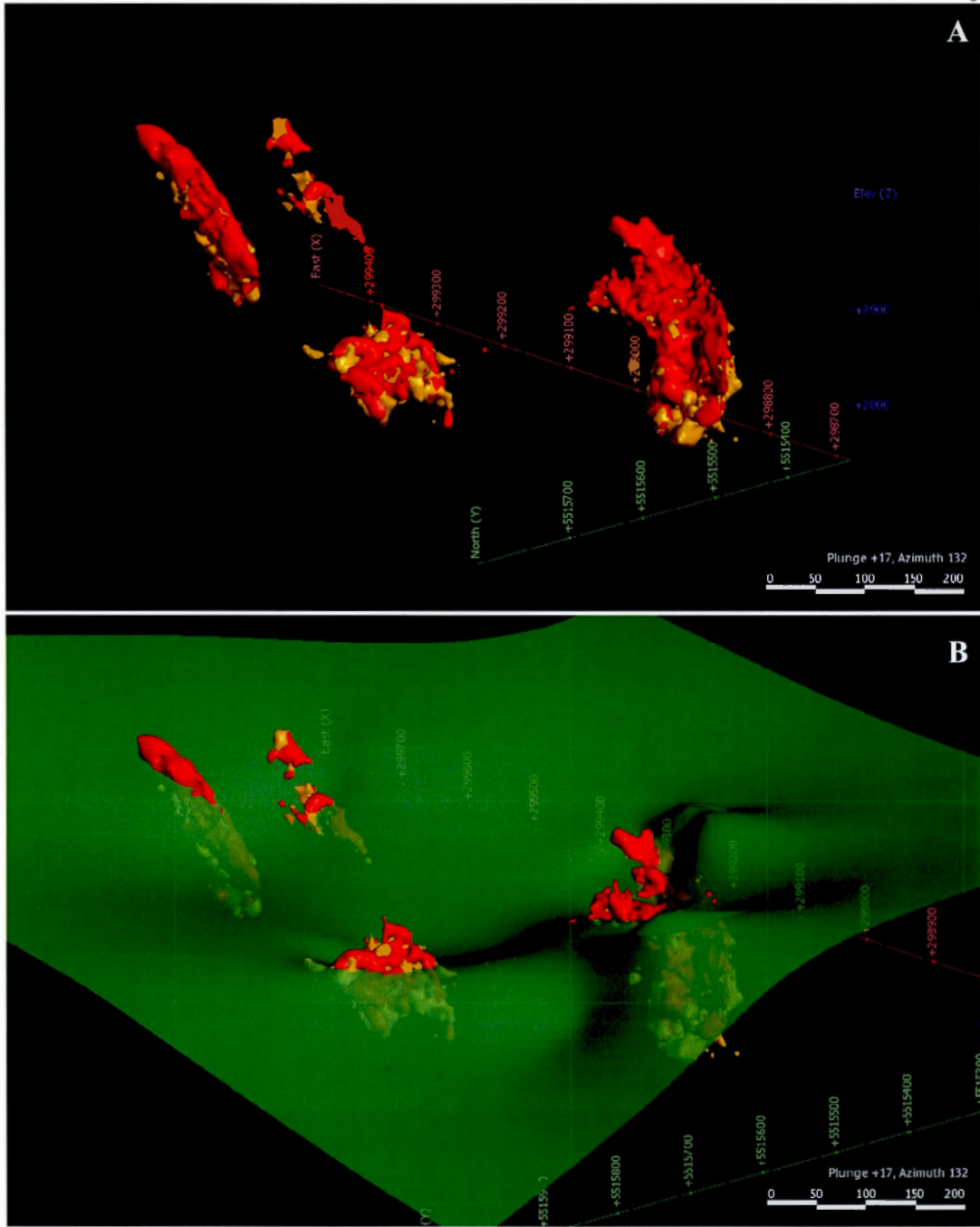


Figure A.4. Visualisation des quatre corps minéralisés vers le SE (N 132) avec Persévérence-Ouest et Equinoxe au premier plan et Persévérance-Main/2 au second plan. (A) Orientation marquée des corps minéralisés. (B) Relation entre les corps minéralisés et la Tuffite Clé. La partie nette des corps minéralisés se situe au dessus du niveau de Tuffite Clé. A noter la dépression apparente marquée par le plan de la Tuffite Clé au centre du gisement.

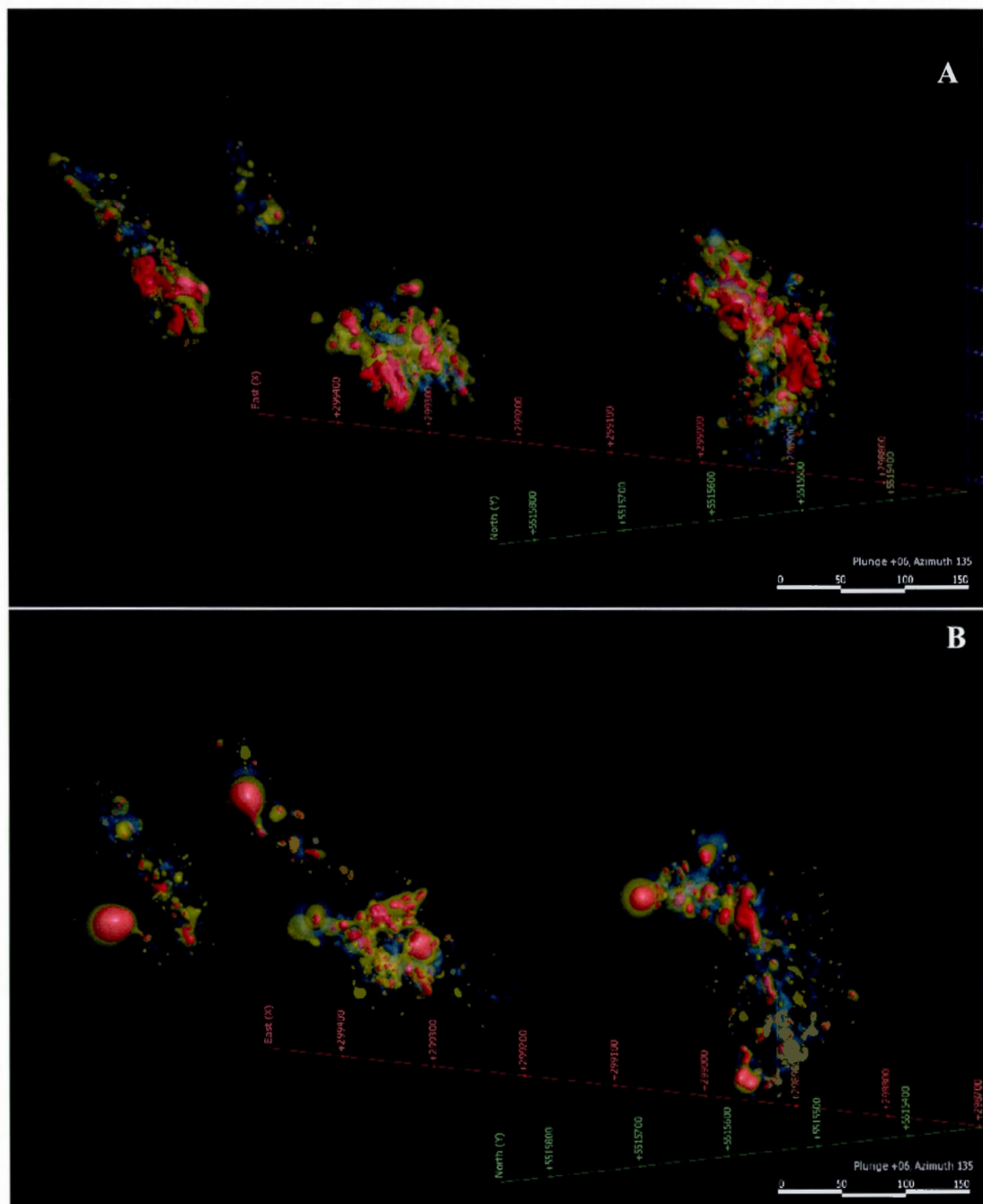


Figure A.5. Distribution métallique des corps minéralisés réalisée à partir des analyses en métaux de base, *vue vers le SE*. (A) Interpolations pour le zinc à 7 % (bleu), 15 % (jaune) et 25 % (rouge). (B) Interpolations pour le cuivre à 1 % (bleu), 2 % (jaune) et 3 % (rouge).

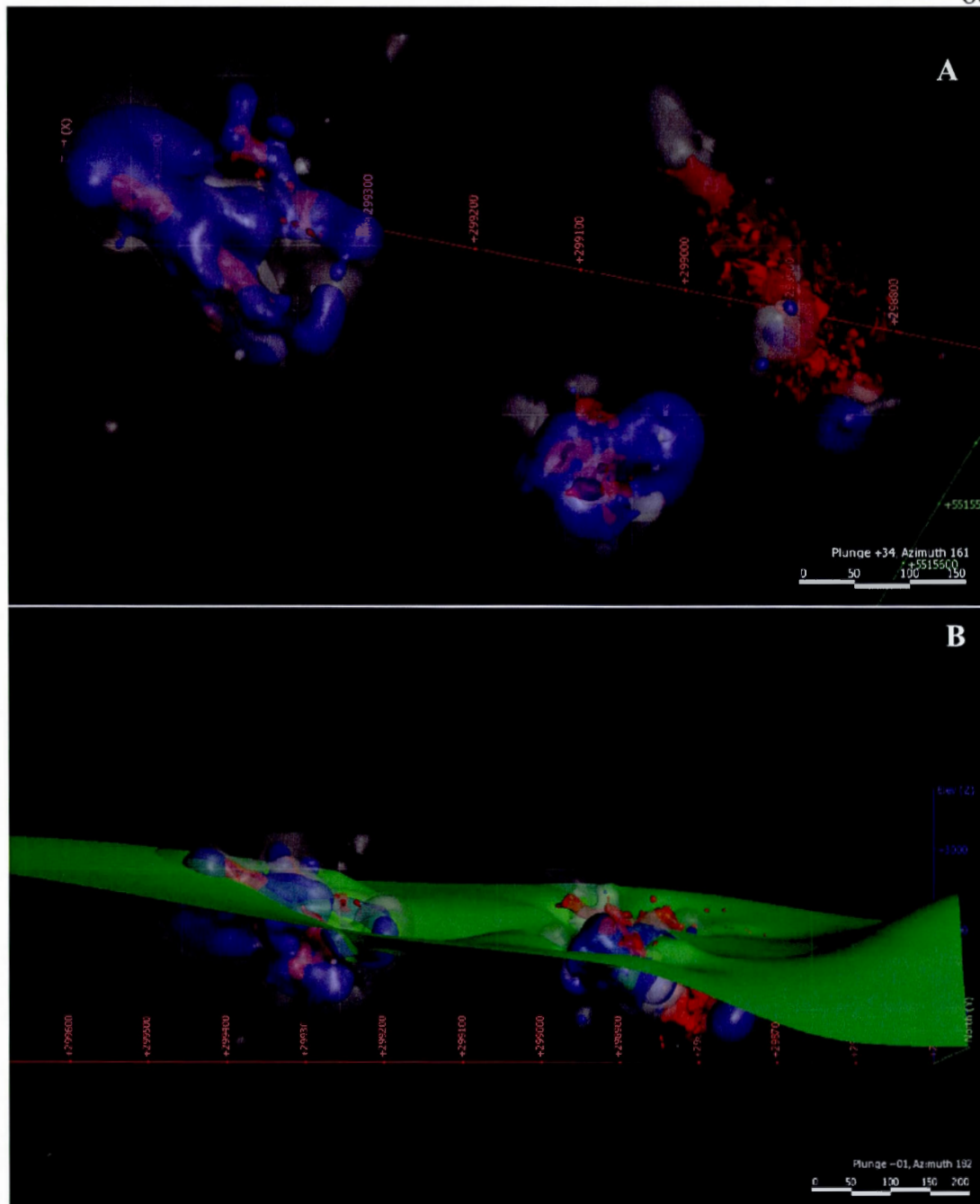


Figure A.6. Distribution 3D des résultats du bilan de masse pour MgO, réalisée à partir des analyses en éléments majeurs. (A) Interpolation des gains de masse en MgO à +10 % (gris) et +12 % (bleu) en relation avec la position des lentilles (rouge), vue vers le SSE. (B) Mêmes résultats en vue de profil (vers le S), montrant la discordance nette par rapport à la Tuffite Clé.

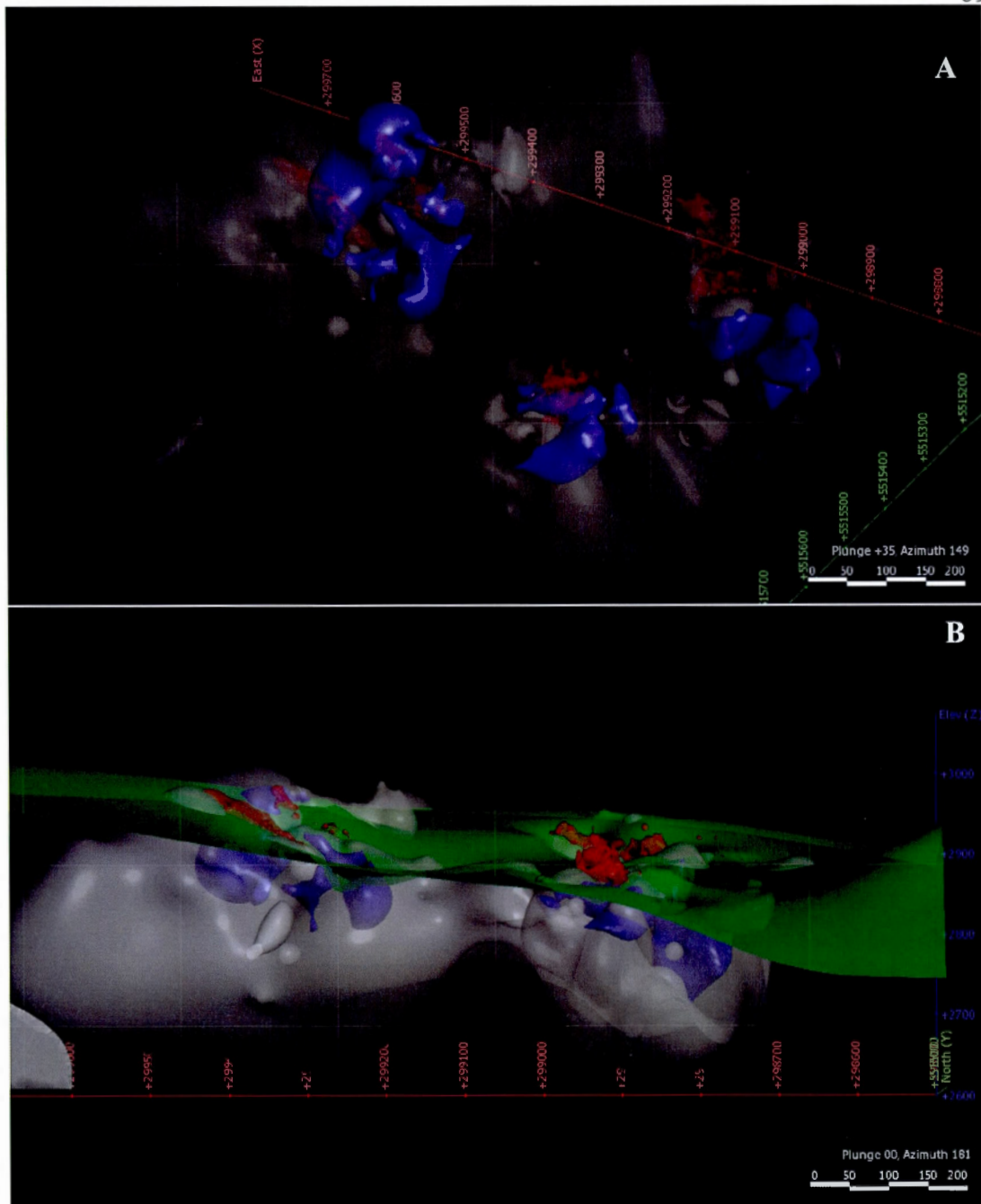


Figure A.7. Distribution 3D des résultats du bilan de masse pour K₂O, réalisée à partir des analyses en éléments majeurs. (A) Interpolation des pertes de masse en K₂O à -1,5 % (gris) et -2 % (bleu) en relation avec la position des lentilles (rouge), vue vers le SSE. (B) Mêmes résultats en vue de profil (vers le S), montrant la discordance par rapport à la Tuffite Clé.

La modélisation 3D aide à identifier les paramètres qui influencent la minéralisation au sein du gisement de Persévérence. Elle illustre en particulier l'attitude verticale des corps minéralisés, perpendiculaire à la séquence volcanique qui elle est sub-horizontale (matérialisée par la rhyolite de Watson, le Tuffite Clé et la rhyodacite de Dumagami). Les quatre lentilles montrent par ailleurs un aplatissement marqué et une orientation globale est-ouest. D'autre part, le modèle aide à clarifier la relation entre la Tuffite Clé et les lentilles minéralisées en soulignant que la partie sommitale des sulfures massifs recoupe le plan de l'horizon marqueur. La modélisation met aussi en valeur la présence d'une possible dépression à la base de le rhyodacite de Dumagami, qui avec les épaisseurs variables de cette dernière, pourrait caractériser une structure en dôme de l'unité. Les bilans de masse pour MgO et K₂O montrent respectivement des gains et des pertes de masse distribués dans la rhyolite de Watson (mur de la minéralisation) et dans la rhyodacite de Dumagami (toit de la minéralisation).

BIBLIOGRAPHIE

- Adair, R. 2009. «Technical report on the resource calculation for the Bracemac-McLeod discoveries, Matagami, Quebec» *National Instrument 43-101, Donner Metals Ltd.*, 194 p.
- Arnold, G., 2006, Feasibility study update of the Perseverance project, Matagami, Quebec: Falconbridge Limited, 178 p.
- Genna, D., D. Gaboury, et G. Roy. 2013. «The Key Tuffite, Matagami Camp, Abitibi Greenstone Belt, Canada: petrogenesis and implications for VMS formation and exploration» *Mineralium Deposita*, vol. 49, p. 489-512.
- Hannington, M.D., C.T. Barrie, et W. Bleeker. 1999. «The Giant Kidd Creek Volcanogenic Massive Sulfide Deposit, Western Abitibi Subprovince, Canada: Preface and Introduction in Einaudi, M. T., ed., The Giant Kidd Creek Volcanogenic Massive Sulfide Deposit, Western Abitibi Subprovince, Canada» *Economic Geology Monograph*, vol.10, p. 1-30.
- Ioannou, S., et E. Spooner. 2007. «Fracture analysis of a volcanogenic massive sulfide-related hydrothermal cracking zone, Upper Bell River Complex, Matagami, Quebec: application of permeability tensor theory» *Economic Geology*, vol. 102, p. 667-690.
- Lavallière, G., J. Guha, et R.Daigneault. 1994. «Cheminées de sulfures massifs atypiques du gisement d'Isle-Dieu, Matagami, Quebec; implications pour l'exploration» *Exploration and Mining Geology*, vol. 3, p. 109-129.
- Piché, M., J. Guha, et R. Daigneault. 1993. «Stratigraphic and structural aspects of the volcanic rocks of the Matagami mining camp, Quebec; implications for the Norita ore deposit» *Economic Geology*, vol. 88, p. 1542-1558.
- Roberts, R.G. 1975. «The geological setting of the Mattagami Lake Mine, Quebec; a volcanogenic massive sulfide deposit» *Economic Geology*, vol. 70, p. 115-129.
- Ross, P.-S., V.J. McNicoll, J.-A. Debreil, et P. Carr. 2014. «Precise U-Pb Geochronology of the Matagami Mining Camp, Abitibi Greenstone Belt, Quebec: Stratigraphic Constraints and Implications for Volcanogenic Massive Sulfide Exploration» *Economic Geology*, vol. 109, p. 89-101.